Chem Soc Rev

REVIEW ARTICLE

View Article Online
View Journal | View Issue

Cite this: Chem. Soc. Rev., 2023, 52, 6191

Perspectives on recent advancements in energy harvesting, sensing and bio-medical applications of piezoelectric gels

Thangavel Vijayakanth,[a] Sudha Shankar,[ac] Gal Finkelstein-Zuta,[ab] Sigal Rencus-Lazar,[a] Sharon Gilead[ac] and Ehud Gazit *[ab]

The development of next-generation bioelectronics, as well as the powering of consumer and medical devices, require power sources that are soft, flexible, extensible, and even biocompatible. Traditional energy storage devices (typically, batteries and supercapacitors) are rigid, unrecyclable, offer short-lifetime, contain hazardous chemicals and possess poor biocompatibility, hindering their utilization in wearable electronics. Therefore, there is a genuine unmet need for a new generation of innovative energy-harvesting materials that are soft, flexible, bio-compatible, and bio-degradable. Piezoelectric gels or PiezoGels are a smart crystalline form of gels with polar ordered structures that belongs to the broader family of piezoelectric material, which generate electricity in response to mechanical stress or deformation. Given that PiezoGels are structurally similar to hydrogels, they offer several advantages including intrinsic chirality, crystallinity, degree of ordered structures, mechanical flexibility, biocompatibility, and biodegradability, emphasizing their potential applications ranging from power generation to bio-medical applications. Herein, we describe recent examples of new functional PiezoGel materials employed for energy harvesting, sensing, and wound dressing applications. First, this review focuses on the principles of piezoelectric generators (PEGs) and the advantages of using hydrogels as PiezoGels in energy and biomedical applications. Next, we provide a detailed discussion on the preparation, functionalization, and fabrication of PiezoGel-PEGs (P-PEGs) for the applications of energy harvesting, sensing and wound healing/dressing. Finally, this review concludes with a discussion of the current challenges and future directions of P-PEGs.

Received 20th April 2023

DOI: 10.1039/d3cs00202k

rsc.li/chem-soc-rev

1. Introduction

Flexible, soft, wearable and self-powered electronic devices have recently emerged as promising candidates for potential applications in next-generation portable and smart electronic technologies.[1–7] Currently, the main approach to powering commercial electronics primarily relies on the use of conventional energy storage systems such as batteries and capacitors.[8–12] However, the main drawbacks of these systems are their rigid configuration, lack of long-term stability, and larger area device structure, which limit their capacity to meet the requirements for smart, flexible and self-powered electronics. Additionally, with the advancement of the fast-growing industrial revolution and global energy consumption, new development of electronic devices based on renewable energy technologies is required to fulfill the power energy sources for our daily life. Unlike non-renewable energy resources such as natural gas, coal, petroleum, oil, metal ores and earth minerals, which are only available for a finite time, mechanical energy is highly abundant and can serve as basis to fabricate extremely useful natural energy sources.[13–16] Traditional piezoelectric energy harvesters/sensors based on perovskite inorganic ceramic oxides (lead titanate, $PbTiO_3$; barium titanate, $BaTiO_3$; lead zirconium titanate, $PbZrTiO_3$; sodium bismuth titanate, $BiNaTiO_3$), piezoelectric polymers (poly-vinylidene fluoride, PVDF; tri-fluoroethylene, TrFE; hexafluoropropylene, HFP; tetrafluoroethylene, TeFE; chlorotrifluoroethylene, CTFE; polyamides, PA; polyesters, PE; polyurethane, PUR; polyacrylonitrile, PAN) and other piezoelectric materials (zinc oxide, ZnO; zinc sulfide, ZnS; cadmium sulfide, CdS; aluminum nitride, AlN; gallium nitride, GaN and indium nitride, InN; tin monosulfide, SnS; molybdenum disulfide, MoS_2 and tungsten diselenide, WSe_2, *etc.*) are proven to show excellent output device performances due to their high piezoelectric properties.[17–24]

[a] *Shmunis School of Biomedicine and Cancer Research, George S. Wise Faculty of Life Sciences, Tel Aviv University, Tel Aviv-6997801, Israel*
[b] *Department of Materials Science and Engineering, Iby and Aladar Fleischman Faculty of Engineering, Tel Aviv University, Tel Aviv-6997801, Israel. E-mail: ehudg@post.tau.ac.il*
[c] *Blavatnik Center for Drug Discovery, Tel Aviv University, Tel Aviv-6997801, Israel*

In addition, conventional piezoelectric materials have found considerable commercial applications in capacitors, actuators, sensors, buzzers, grill igniters, diesel fuel injectors, acoustic guitar pickups, ultrasonic transducers, thermoelectrics, photovoltaics and memory devices.[25–28] However, these materials pertain to certain limitations to obtaining the active piezoelectric phase and pose serious environmental concerns, such as the presence of toxic lead (Pb) and high heavy metal concentration, high density, high ductility, and high-temperature synthesis, which prevent the use of these materials in flexible and wearable electronic technologies.[29–32]

Recently, numerous efforts were made to produce flexible and green power sources for bio-electronic applications.[33–38] Piezoelectric generator (PEG) or piezoelectric energy harvester (PEH) comprise a newly developed technology allowing simple and effective generation of electromechanical energy to be achieved *via* a wide range of bio-mechanical movements, such as bending, folding and stretching motions of human-body activities.[39–43] Very recently, PEGs based on supramolecular organic and hybrid organic–inorganic materials were extensively explored due to their facile synthesis, lightweight, mechanical flexibility, structural tunability, topological adaptability, multifunctionality, low-temperature processability, easy orientation of molecular dipoles, efficient charge transport, and ease of device fabrication, which are essential for the production of low-cost and multi-functional powered devices.[44–49] The

Thangavel Vijayakanth

Thangavel Vijayakanth received an MSc from the Bharathidasan University, India, and a PhD in Chemistry from the Indian Institute of Science Education and Research (IISER), Pune, India, in 2020 with Prof. Ramamoorthy Boomishankar. His PhD dissertation was titled "Organo and amino phosphonium cation-derived ferro- and piezoelectric materials and their utility in mechanical energy harvesting applications". He subsequently joined Tel-Aviv University, Israel, in 2021 for his postdoctoral studies and is currently working with Prof. Ehud Gazit. His current research interests embrace the molecular self-assembly of amino acids and short-peptides, focusing on bio-piezoelectric applications such as energy harvesting, sensing, self-powered, implantable and wearable electronics.

Sudha Shankar

Sudha Shankar received her MSc in Pharmaceutical Chemistry from Banasthali University, Rajasthan, India. She completed her PhD in 2020 from CSIR-Indian Institute of Integrative Medicine, Jammu, India. Her PhD studies focused on the synthesis and conformational studies of αβ/αγ hybrid peptides and biological evaluation as antimicrobial and anticancer agents. She then joined as a Newton International Postdoctoral Fellow at the University of Glasgow, Scotland, UK, focusing on "Total synthesis of Bottromycin using Solid Phase Peptide Synthesis". Currently, she is working with Prof. Ehud Gazit's group in the Medicinal Chemistry Unit of the Blavatnik Center for Drug Discovery, Tel Aviv University, as Postdoctoral Fellow. Her current research interests focus on the design, synthesis and self-assembly of biologically active peptides to explore their multifaceted applications ranging from sustainable energy to healthcare systems.

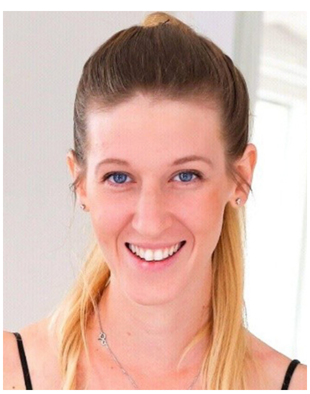

Gal Finkelstein-Zuta

Gal Finkelstein-Zuta is currently a PhD student under the supervision of Prof. Ehud Gazit's group at both the Shmunis School of Biomedicine and Cancer Research, George S. Wise Faculty of Life Sciences, and the Department of Materials Science and Engineering, Tel Aviv University, Israel. She also obtained her MSc, from Tel Aviv University, under the supervision of Prof. Dan Peer. Prior, she completed a BSc Dual degree in Chemistry and Chemical Engineering from Ben-Gurion University of the Negev, Israel. Her research focuses on unique bio-inspired self-assembled short peptide structures, especially ones with piezoelectric properties.

Sigal Rencus-Lazar

Sigal Rencus-Lazar joined Prof. Ehud Gazit's group in 2017 as a scientific writer and editor. She is involved in various research fields in the lab, including metabolite self-assembly, inborn error of metabolism disorders, neurodegenerative diseases, and peptide nanotechnology. Dr Rencus-Lazar completed her BSc, MSc (both summa cum laude), and PhD studies at The George S. Wise Faculty of Life Sciences at Tel Aviv University, Israel.

multifaceted benefits of newly emerging supramolecular materials are considered to provide an alternative to traditional materials due to their facile solution processability and ease of device fabrication. Despite several advantages, however, most of the non-bioorganic and hybrid organic–inorganic supramolecular materials have various disadvantages, including the lack of intrinsic chirality, biocompatibility and bio-degradability, which hinders their piezoelectric properties and potential use in self-powered and portable electronic applications.

In this context, bio-inspired or bio-supramolecular materials are desired since they display biosafety, biocompatibility, biodegradability, strong hierarchical self-assembly behavior and inherent chirality, important parameters for materials to be used in bio-piezoelectric energy harvesting technologies.[50–54] Recently, we and others have shown that PEGs based on biocompatible amino acids, peptides and proteins revealed output characteristics, such as output voltage, output current, current density and power density, comparable to several of the traditional and non-bioorganic supramolecular piezoelectric energy harvesting materials.[55–61] Such non-toxic, biocompatible and eco-friendly PEGs have emerged as a new paradigm shift for the development of next-generation programmable and smart electronic systems. Other well-studied traditional bio-piezoelectric materials, such as wood, bone, silk, collagen, chitin, chitosan, elastin, cellulose, clamshell, alginate, virus and eggshells, were highlighted and comprehensively discussed in many research articles.[62–69]

To date, great efforts have been dedicated to the generation of piezoelectric devices based on biomaterials that are soft, self-powered, stretchable, flexible, lightweight and have ease of device fabrication characteristics. However, flexibility and stretchability are often sacrificed due to their complex device architectures.[70] In this context, hydrogels, three-dimensional (3D) polymeric structures build of cross-linked hydrophilic networks, are considered intriguing candidates for the development of flexible electronics owing to their excellent biocompatibility and flexibility.[71,72] Additionally, hydrogels are excellent substrate candidates for the application of adaptable and bio-medical systems since they can mimic the natural tissue extracellular matrix (ECM) and are soft, flexible, breathable, water-rich, can be readily used to detect mechanical deformation, and are appropriate for cell signaling.[73–75]

In recent years, the combination of hydrogels with piezoelectric properties has received great attention in flexible electronics and healthcare technologies.[76,77] Moreover, they also possess several advantages including high transparency, intrinsic chirality, good deformability, extreme soft-ability, good flexibility, excellent stretchability, and superior biocompatibility characteristics, making them a promising option for utilization in piezoelectric electronics and wearable technology.[78] Additionally, the aforementioned highly attractive characteristics make hydrogels similar to natural tissues, allowing their function as piezoelectric materials. In addition, non-centrosymmetric structure, polar orientation and asymmetric crystalline structures are essential for hydrogels to show piezoelectric properties. Importantly, in contrast to hydrogels, conventional components of piezoelectric devices lack the ductility and stretchability required for flexible and wearable electronics. Thus, the piezoelectric properties of hydrogels have opened new possibilities for customized design and their applications in flexible and portable electronics.

PiezoGel is part of a larger family of smart crystalline piezoelectric materials, which generate electricity in response to mechanical stress or deformation. PiezoGel is very similar to hydrogel or soft solid composed of a network of crosslinked

Sharon Gilead

Sharon Gilead was the head of nanotechnology research at Prof. Gazit's research group, where she conducted and lead various research activities. She studied chemistry and biology (double major, cum laude in both) at Tel Aviv University (TAU). She received her MSc (summa cum laude) and PhD (2007) from the Department of Molecular Microbiology and Biotechnology at TAU. Her PhD studies were focused on a molecular-level analysis of amyloidal protein misfolding, protein interactions and self-assembly. She was a post-doctoral fellow at the Department of Electrical Engineering, after which she worked as a researcher at Neurophage Pharmaceuticals (USA) at the Israeli branch in Tel-Aviv, developing drugs against Alzheimer's disease. Currently, she is the Scientific Director of the Blavatnik Center for Drug Discovery at TAU.

Ehud Gazit

Ehud Gazit is a Professor and Endowed Chair at the Shmunis School of Biomedicine and Cancer Research and the Department of Materials Science and Engineering at Tel Aviv University. He received his BSc (summa cum laude) after studying at the Special Program for Outstanding Students at Tel-Aviv University and his PhD (highest distinction) from the Weizmann Institute of Science. He has been a faculty member at Tel Aviv University since 2000, following the completion of his post-doctoral studies at the Massachusetts Institute of Technology, where he also had held a visiting appointment. He also had visiting appointments at Cambridge University, Fudan University, and Umeå University. He was recently appointed as the 2023 International Solvay Chair in Chemistry. His research interests involve exploring biological and bio-inspired molecular self-assembly.

macromolecular hydrophilic polymers with an ordered three-dimensional structure, the majority of which is composed of water molecules within their interlocked molecular network. The advantages of PiezoGel over other types of hydrogel (typically, amorphous hydrogels) are the ordered crystalline and acentric structural features necessary for piezoelectric energy harvesting/sensing and certain bio-medical applications.[76,77,79] Depending on their composition, PiezoGels can be classified as organic, inorganic, or hybrid organic–inorganic compounds. The molecular self-assembly of PiezoGels is primarily driven by the ability to organize ordered structures through various non-covalent interactions, including electrostatic forces, van der Waals contacts, hydrogen bonding interactions, π–π interactions, hydrophobic interactions and host–guest interactions.[77,80,81] In addition, PiezoGel possesses distinctive features, such as intrinsic chirality, high sensitivity, good electroactivity, low symmetry, permanent dipole moment, strong polarization, self-power generation, the superior ability to mimic the natural ECM, and the potential to develop stiffness that resembles biological tissues.[82–84] Thus, all these significant characteristics of PiezoGels make these materials promising candidates for applications in tissue engineering, self-healing, energy harvesting, light-emitting diode devices, bio-sensing, soft robotics, bio-mechanics, electronic skins, wound healing, drug delivery systems, and medical devices (Fig. 1).[85]

Fig. 1 Schematic diagram showing the development of P-PEGs. The main applications of P-PEGs are covered in this review based on the coupling of flexible electronics and piezoelectric properties. The diverse applications of P-PEGs showing sensing (a, top panel), artificial electronic skin (AES) (b, upper right panel), light-emitting diode (LED) devices (c, lower right panel), tissue engineering (d, bottom panel), energy harvesting (e, lower left panel) and wound healing (f, upper left panel).

In this review, we provide an overview of the recently emerging examples of PiezoGel-PEGs (P-PEGs) comprised of ceramic oxides, polymers and supramolecular piezoelectric materials used for energy harvesting, sensing and wound dressing. Furthermore, we present a detailed overview of the evolution of PiezoGels from traditional piezoelectric materials such as perovskite ceramic oxides to piezopolymers to supramolecular materials. Though piezoelectricity was already observed a century ago for Rochelle salt and potassium dihydrogen phosphate,[79,86,87] we explain why new emerging materials are still needed. In particular, we focus on the possible applications of PiezoGel in smart, flexible, stretchable and bio-medical electronics applications. Moreover, hydrogels and PEGs have been extensively explored independently, but combining them could be a significant step forward in the development of bio-electronics and human–machine interface technologies. However, to date, as far as we know, there are no comprehensive reviews covering the use of hydrogels for piezoelectric energy harvesting, sensing, wound healing and tissue engineering applications. We hope that this review will not only deepen the ties between smart self-powered and bio-medical technologies but also advance further research and applications of flexible, stretchable and wearable electronics. Finally, we conclude this review with a discussion of the current challenges and future perspectives for the emergence of PiezoGel-based portable wearable electronics.

2. Fundamentals of piezoelectric generators

Dielectric materials are electrically insulating systems that can be polarized by an applied electric field. These materials display electric polarization when positively charged nucleus and negatively charged electrons move towards and opposite directions of the applied electric field. Dielectrics are mainly grouped into two distinct categories: non-polar or linear and polar or non-linear dielectric materials. Piezo-, pyro-, and ferro-electric materials belong to the category of non-linear dielectric substances due to the presence of non-centrosymmetric structure and permanent electric dipole moment.[88] Among these, piezoelectric materials, the focus of this review, are highly attractive owing to the minimal structural prerequisites and ease of applicability.[89] Moreover, the lack of a centrosymmetric structure or inversion symmetry is essential to exhibit piezoelectric properties in crystalline materials. According to the definition, out of the 32 possible crystallographic point groups and 230 space groups, piezoelectric materials must adopt one of the 21 non-centrosymmetric point groups (apart from 432), while the remaining 11 point groups are classified as centrosymmetric classes.[90]

Piezoelectricity was first discovered by Pierre and Jacques Curie in 1880 and it can be observed in certain materials which feature a polar axis without a center of crystal symmetry.[91–93] The displacement theory of Maxwell, which serves as the scientific foundation for PEGs, is based on the mechanisms inducing an electric charge by mechanical stress (direct piezoelectric effect) and change in dimensions when an electric field is applied across the material (indirect or converse piezoelectric effect).[94,95] The typical piezoelectric coefficient (d_{33}) of the material is used to quantify the piezoelectric performance and is expressed as either C N^{-1} (coulombs per Newton) or m N^{-1} (meter per Newton).[96,97] The principle of operation of a P-PEG device relies on a direct piezoelectric effect, namely when an external mechanical pressure is applied to a piezoelectric material, the polarized dipole density of the P-PEG device increases correspondingly. To maintain charge balance, electrons concurrently move across an external circuit from the bottom electrode to the top electrode. When the external force is removed, the typical P-PEG device returns to its original state, resulting in a decrease in polarised density and a movement of electrons from the top to the bottom of the electrode. In a typical experiment, by connecting the display system (usually, an oscilloscope) to the external circuit, the alternating electrical signals can be read out. Fig. 2 shows a typical mechanism of charge generation due to applied mechanical stress (direct piezoelectric effect, left) and strain induced by the application of an external electric field (converse piezoelectric effect, right). PEGs typically consist of a piezoelectric material (in this case, PiezoGel) and two electrodes connected on both sides. When mechanical stress is applied to the PEG, a net dipole moment and its electrical polarization properties are generated, owing to the non-linear arrangement of PiezoGel materials (Fig. 2a and b). The resulting electric dipoles align in one direction due to the potential difference between the electrodes, which allows the current to flow through an external circuit from the top to bottom electrodes. The efficiency of the electromechanical energy-generating performance depends on several factors, such as the material type (inorganic ceramic oxides, single crystals, polymers, composites and hydrogels), materials dimensions (width, length and thickness), and other key parameters (direction of applied force, choice of the electrode, active surface area between electrode and material, the magnitude of the mechanical force, applied frequency, water content and the structural morphological alignment of the piezoelectric materials).[98–100] The typical P-PEGs output voltage and current signals as a function of time are schematically represented in Fig. 2c and d. Given the advantages of PEGs that can convert ambient mechanical energy into electricity, PEG-based hydrogels have been recently explored owing to their intrinsic non-centrosymmetric crystalline phase, structural tunability and biocompatibility. As a result, research of piezoelectric hydrogels based on PEGs have been fast growing aiming to overcome an energy crisis and enable cost-effective biomedical applications.[76]

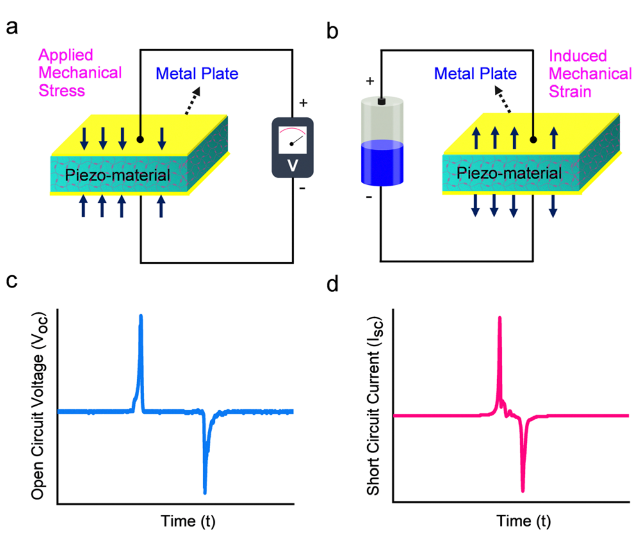

Fig. 2 Fundamentals of PEGs. (a) and (b) Schematic representation displaying the working mechanism of (a) direct and (b) converse piezoelectric effect. (c) and (d) Typical piezoelectric output (c) voltage and (d) current curves.

3. Advantages of PiezoGels as PEGs

This section emphasizes the substantial benefits of using hydrogel materials for the fabrication of highly flexible and stretchable PEGs. Further consideration is given to the advantages of fabricating piezoelectric hydrogels-based P-PEG devices.

3.1 Transparency

Transparent hydrogels/PiezoGels are key components for developing next-generation and portable device applications such as mobile phones, contact lenses, smart windows, soft robotics, optical signaling, ultrasound imaging, optical coatings, electronic skins, wound dressings, *etc.* (Fig. 3a and b).[101–107] High-transparency PEGs are far more desirable than traditional low-transparency PEGs due to their simple and easy integration into diverse seamless optoelectronic device applications without compromising their visibility. To achieve high transparency, the water content of the pre-polymerization mixture should not exceed the amount of water absorption into the hydrogel to prevent phase separation, which typically results in opaque characteristics. Taking advantage of their transparency, PiezoGels provide an invaluable tool in the basic research of various biological tissues, with the establishment of organoid structures allowing to mimic the organization and processes taking place *in vivo* in the corresponding organ. Very recently, Zhao and coworkers developed a transparent bioadhesive ultrasound (BAUS) device, which consists of a rigid piezoelectric probe adhered to the skin composed of a hydrogel-elastomer hybrid which is soft, robust, anti-dehydrating, and biocompatible.[108] The BAUS device provided continuous accessibility to ultrasound imaging, including the carotid artery, blood vessels, heart, muscle, and lung. In addition, they also demonstrated that the transparent BAUS probe could successfully transmit ultrasound waves, protect it from skin deformation, and maintain a stable and comfortable bonding with the skin over 48 hours. Thus, good transparency could make it easy for doctors to diagnose the organoid cultures corresponding to diverse organs, including the pancreas, eye, kidney, brain, and gastrointestine.[109,110] Therefore, the integration of high transparency with other characteristics, especially flexibility, will be crucial in the future to realize the potential utilization of PiezoGels in pressure sensors, prosthetic skins, and optoelectronic device applications.

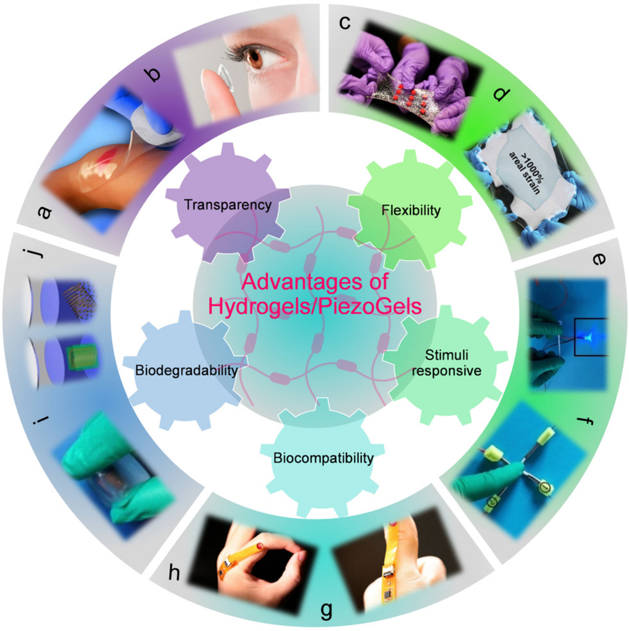

Fig. 3 Advantages of hydrogels/PiezoGels in energy and biomedical applications. (a) Photograph of the polyvinylpyrrolidone (PVP), polyethylene oxide (PEO) and agar-based transparent hydrogel. Reproduced with permission. Copyright © 2007, HMP Communications, LLC. (b) Photograph of a contact lens-based transparent hydrogel. Reproduced with permission. Copyright © 2023, Wigram & Ware Opticians. (c) and (d) Photograph of an extremely tough, stretchable and flexible hydrogel elastomer. Reproduced with permission.[119] Copyright © 2017, American Association for the Advancement of Science. (e) and (f) Photograph of the stimuli-responsive PVA-soluble starch composite gel. Reproduced with permission.[148] Copyright © 2021, WILEY-VCH Verlag GmbH & Co. KGaA, Weinheim. (g) and (h) Photograph of a bio-compatible and wearable sensor based on DNA hydrogel. Reproduced with permission.[165] Copyright © 2021, American Association for the Advancement of Science. (i) and (j) Optical images of a flexible and biodegradable bacterial cellulose-neodymium magnet (BC-NdFeB) composite material. Reproduced with permission.[174] Copyright © 2022, Elsevier Ltd.

3.2 Flexibility and stretchability

Flexibility and stretchability are two other important characteristics of hydrogels and PiezoGels for applications in rollable displays, conformable sensors, electronic eye cameras, mechanically formable-deformable devices, and human–machine interface monitoring systems.[111–117] To develop a soft interface with biological tissues, it would be extremely advantageous for hydrogels and piezoelectric materials to display a combination of desirable properties including softness, flexibility, deformability, and biocompatibility. Recent studies on hydrogels/PiezoGels demonstrate attractive flexibility, stretchability, and superior fracture resistance; notable examples are highly robust and stretchable DNA-based gels,[118] poly(2-hydroxyethyl methacrylate, PHEMA),[119] polyvinyl alcohol (PVA),[119] acrylic acid-2-ureido-4-pyrimidone (UPy),[120] polyacrylamide (PAM)-alginate,[121] PAM-hyaluronic acid,[122] PAM-chitosan,[122] silk fibroin-tannic acid[123] and so on. Recently, Kaltenbrunner and coworkers developed a hybrid of elastomer and ionic hydrogels that could endure a biaxial strain higher than 2000%, demonstrating the high stretchability, superior robustness, and high-fatigue resistance properties desired for the development of soft sensors, health monitoring wearables, and elastic electronics (Fig. 3c and d).[119] Furthermore, when bonded to the elastomer, these hydrogels were stretched by more than 1000% without delamination (Fig. 3d). It is particularly advantageous to produce flexible and stretchable PEGs to harvest biomechanical energy from a simple action of tiny bio-mechanical human body movements such as bending, folding, twisting, and stretching.[124–126] Therefore, there is a need for the development of flexible and stretchable PEGs systems based on piezoelectric hydrogels that can sense pressure and have a wide range of potential applications in the field of electronic skin.

3.3 Stimuli-responsiveness

The stimuli responsiveness of hydrogels/PiezoGels is one of the key characteristics that influence their use in biological and pharmaceutical fields.[127–129] Smart hydrogel systems containing a variety of physiologically and structurally responsive components adapt to environmental stimuli such as pH, temperature, light, humidity, solvent composition, ionic strength, pressure, ultrasonic, shear stress, electrical fields, magnetic fields, and chemicals.[130–138] Significant advances in stimuli-responsive hydrogels have been demonstrated, including use as functional mediums for actuators, detectors, sensors, and biomedical applications such as green surfactants, artificial muscles, drug delivery, tissue engineering, and cell imaging.[139–142] Electrically or magnetically stimulated hydrogels should show key properties such as precisely tunable signal amplitude, frequency, and controlled polarization alignment direction. Such responsiveness to the magnetoelectric field allows the alignment of the polarization direction of the hydrogels and strengthens the piezoelectric outputs and other properties of hydrogels which are useful for applications in the fields of bio-electronics and healthcare.[143–147] Recently, Gong and coworkers investigated PVA-soluble starch and thermoplastic polyurethane (TPU) encapsulated composite hydrogels as elastic conductors for magnetoionic induction sensing, strain sensing and piezoelectric sensing (Fig. 3e and f).[148] The developed hydrogel generated an alternating magnetic field, which induced an electric field in the hydrogel, allowing free ions to flow in the same direction, resulting in an ionic current. Moreover, the designed hydrogels functioned as a PiezoGel sensor when tapped with a human finger, producing an output voltage of 0.4 mV, demonstrating their utilization as a P-PEGs-based electronic skin sensor. Fig. 3e and f illustrate an encapsulated TPU with a PVA-soluble starch composite PiezoGel that shows a strong electrical response and piezoelectric sensing. Such a material served a crucial role in the development of a stimuli-responsive flexible sensor for application in cutting-edge and smart textile technologies.[76]

3.4 Biocompatibility

Bio-compatible hydrogels are highly desirable for the design of a piezoelectric gel-based PEG for its applicability in healthcare and bio-electronics applications.[149,150] In this context, hydrogels displaying superior bio-functionality and bio-safety characteristics were explored as promising biomaterials for a multitude of applications such as tissue engineering, bio-sensing, wound-dressing, self-recuperating, health-monitoring, regenerative medicine, drug-delivery systems, artificial contact-lens, bio-adhesives, and biomedical microelectromechanical devices.[151–159] Hydrogels, particularly DNA-based materials, have received a lot of attention due to their high biological recognition, good electrical transport, piezoelectricity properties, and intrinsic biocompatibility.[160–164] For example, Ho and coworkers developed a wound infection sensor comprised of DNA hydrogel, which demonstrated excellent biocompatibility, permittivity tunability, capacitive sensing, wireless and battery-free characteristics making them highly suitable for bio-sensing in clinical technology applications (Fig. 3g and h).[165] This new sensor device allowed wireless detection of clinically significant levels of *Staphylococcus aureus* in a mouse wound model prior to the appearance of infection. In addition, it also revealed good bio-degradability by a deoxyribonuclease (Dnase) enzyme, secreted by certain types of commensal bacteria. As shown in Fig. 3g and h, the DNA hydrogel showed bio-sensing capabilities when mounted on the human body surface by wound dressings, exhibiting a wide range of read-out sensing coverage from 0 to 100%. Therefore, the field of bio-electronics demands such a highly biocompatible hydrogel sensor to construct future smart medical and clinical workspaces.

3.5 Biodegradability

The most important attribute of hydrogels/PiezoGels is their biodegradability, which provides an environmentally benign nature and supports the development of materials for applications in wearable electronics, agriculture, and biomedicine without environmental hazards.[166–170] Since many practical applications require biodegradability, materials employed for the fabrication of P-PEGs should incorporate various features such as the use of non-toxic raw materials, the avoidance of toxic chemicals, the ability to degrade under ambient conditions, the formation of non-toxic substances after degradation, the extent of degradability, and the ease of recyclability.[171–173] Recently, Yang and coworkers developed a compressible, biodegradable and recyclable bacterial cellulose-neodymium magnet (BC-NdFeB)-based hydrogel-PEG for energy harvesting applications (Fig. 3i and j).[174] The PEG device displayed good viscoelastic mechanical characteristics due to the easy compression and recovery deformation. Based on the electromagnetic induction phenomena, the magnetized hydrogel-based magnetoelectric (ME) composites can transform ambient mechanical forces into electrical output during repeated compression and recovery. By applying a periodic force on the PEG device resulted in the maximum output voltage response of 14.5 μV. In addition, the fabricated hydrogel-based energy harvester revealed excellent biodegradability characteristics in enzyme (within 3 h) and water (49 days) phosphate-buffered saline solution, indicating the PEG device degradability in enzymatic degradation is much faster than natural degradation (Fig. 3j). Such biodegradability is highly beneficial in the design and application of P-PEGs in wearable and healthcare applications.

4. Flexible electronic and bio-medical applications of P-PEGs

Flexible and stretchable P-PEG materials are emerging components for self-powered sensing/monitoring and charging/powering electronics. In addition, they can also be utilized for a variety of adaptable electrical and wearable applications, such as human–machine interfaces, tissue engineering and wound healing/dressing. This section discusses the potential limitations of employing traditional materials for energy harvesting, sensing, and wound healing applications and highlight the advantages of fabricating piezoelectric hydrogels-based P-PEG devices.

4.1 PiezoGels for energy harvesting and sensing applications

Energy harvesting is the approach of collecting energy from natural sources, such as heat, light, wind, fluid flow and vibration and converting it into electrical energy that can be effectively stored, transferred, and used to instantly power electric components. The quest for a practical solution that alters the conventional structure of energy supply has been at the forefront due to the increasing demand and depletion of constrained fossil energy resources.[175,176] From the standpoint of sustainability and high efficiency, piezoelectric energy harvesters and sensors have gained significant interest due to their self-powered capability and potential applications in several electronic and wearable or portable devices.[177] Piezoelectric energy harvesters are also promising candidates for autonomous biomedical applications since they can harvest ambient mechanical energy into electrical energy *via* the forces derived from pressure, bending, folding, oscillation and stretching motions of human body functions.[178] As a result, the applications of piezoelectric energy harvesting materials have greatly expanded across a wide range of fields including sensors, capacitors, actuators, motors, printers, memory devices, portable electronics, micro-electro-mechanical-systems and medical implants.[179,180] Piezoelectric sensors may generate a self-powered response by applying mechanical stimulation, unlike traditional sensors which depend on an external power source to function.[181] For this reason, piezoelectric sensors are in high demand in various fields including smart homes, biomedical robotics, human–machine interfaces, animal sensory systems, and health-monitoring systems. In addition, piezoelectric energy harvesting and sensing devices are structurally simple, compact, light-weight, stable and very sensitive to any small strains.[182,183] Over the years, the known piezoelectric energy harvesting and sensing materials, including inorganic ceramics, polymers, composites, supramolecular crystals and powdered crystallites, were developed for different applications due to the excellent piezoelectric polarization. While these piezoelectric materials are widely used for energy harvesting and sensing, the fabrication of soft, stretchable, light-weight and wearable devices is still challenging since these piezoelectrics mainly consist of stiff crystalline structures.[184–189]

In this context, hydrogels composed of piezoelectric components could be ideal candidates owing to their softness, flexibility, deformability, and biocompatibility, all of which are highly desirable for quick response to external triggers and mimicking the ECM of biological tissues.[190] Based on these advantages, the exploration of piezoelectric hydrogels is of growing interest since they are biocompatible, stretchable and can stimulate endogenous "bioelectricity" to promote tissue regeneration and repair.[191] Due to the physical features of hydrogel-based piezoelectrics that mirror biological functions, these characteristics represent a major potential for integrating biological organs and electronics. It has been reported that piezoelectric hydrogels are mechanically robust and adequately stable in various environments allowing to monitor external stimuli such as pressure, strain, temperature, pH, humidity and human-motion sensing *via* electrical signals.[192,193] Therefore, it is crucial to obtain a solid understanding of current progress and advancements of hydrogel-based piezoelectric devices which can be potentially utilized for future generation smart electronics and biomimetic e-skin devices applications. Hence, the piezoelectric properties of hydrogels are appealing, have great potential for the development of flexible, stretchable, self-powered, and wearable electrical stimulation devices featuring applications in energy harvesting and sensing.

4.2 PiezoGels for wound healing/dressing applications

Wound healing refers to the ability of a living organism repair lost or injured tissue. The healing of the skin mainly consists of four stages: hemostasis, inflammation, cell proliferation, and tissue remodeling.[194–196] For a damaged wound to heal successfully, all four stages must take place in the right order and in a predictable time frame. In general, wounds are classified into two types: acute wounds and chronic wounds. Acute wounds often heal quickly and efficiently, while wounds that take a longer time to heal are often classified as chronic wounds due to a delay in one or more stages of the wound healing process.[197–199] Chronic wound healing is affected by various factors that contribute to slow healing, such as unresolved inflammation, infection, neuropathy, poor circulation, a lack of angiogenesis, bio-film formation, and cell proliferation. Additionally, ischemia-reperfusion trauma and nerve regeneration both play an important role in wound healing. Wound dressing is extremely important for wound healing because it cleans, covers, and protects infected wounds from the external environment.[200–205] Numerous types of wound dressings have been used for wound healing, including gauze or cloth, hydrocolloid, foam, transparent film, and hydrogels comprised of natural polymers, peptides and proteins.[206–210] Although traditional wound dressings have been used for wound healing for decades, hydrogels composed of biomaterials have recently been used for non-invasive therapy applications due to their multifaceted advantages of specific biological activity, biocompatibility, antibacterial activity, good non-toxicity or inflammation, excellent biological adhesive behavior, resemblance to soft tissue structure, high-porosity and swelling properties, excellent biochemical and mechanical properties, and high efficacy of providing a quick accelerative, high absorption ability toward exudates and wet permeable environment for wound healing.[211–214] Furthermore, some hydrogel-based dressings can be used as therapeutics, tissue generation systems, and energy harvesters that can mimic the ECM and amplify endogenous bioelectric stimulation, implying their potential application prospects in biomedical and energy systems.[215–217] Taking the aforementioned considerations into account, hydrogels, particularly those showing piezoelectric properties, have great potential as producing bioelectricity systems and wound dressers.

4.3 Polymers-based P-PEGs

Polymeric gels are structurally complex yet soft and flexible materials composed of physically or chemically cross-linked networks with interstitial spaces that can hold water or other liquids while maintaining well-defined structures.[218–221] Polymer gels are three-dimensional networks of diverse shapes and sizes that can deform significantly due to their soft and wet nature. Polymer gels can be produced using a variety of components, which are broadly classified as natural and synthetic polymers.[222–224] Natural polymers used in the development of piezoelectric materials include gelatin, collagen, fibrin, silk, agarose, chitosan, dextran, starch, cellulose, alginate, heparin and hyaluronic acid. Prominent examples of synthetic piezoelectric polymers employed in hydrogel preparation include polyglycerol, sodium polyacrylate, poly acrylic acid, PVA, PAN, PEO, PAM, and other synthetic polymers and copolymers.[225–230] Moreover, piezoelectric polymer gels have multiple advantages including flexibility, stability, permeability, tunable porosity, viscoelasticity, mechanical strength, ease of shape, and ease of production. Furthermore, piezoelectric gels are ideal for a wide range of applications, including pharmaceutical, energy, and medicinal chemistry. A study on a poly(methylacrylic acid) hydrogel, which produced an electric potential under 300 g mechanical stress, was regarded as the first report of piezoelectricity utilizing hydrogel material (Fig. 4a).[231] In this section, we highlight recent findings and the evolving applications of PiezoGels for piezoelectric energy harvesting, sensing and wound dressing or healing applications based on natural or synthetic polymers.

4.3.1 Gelatin-based PiezoGels for energy harvesting. Gelatin is a well-studied natural biopolymer and functional protein derived from collagen, the main structural protein in the ECM. Gelatin, being a collagen derivative product, has similar structural and functional properties.[232–235] Over the years, gelatin-based materials have been extensively explored due to their low cost, non-toxicity, biocompatibility, nonimmunogenicity, biodegradability, as well as attractive chemical and physical features including water solubility, transparency, high tensile strength, and outstanding piezoelectric properties.[236–244]

Ma and coworkers reported the mechanoelectrical properties of soft and wet gelatin gel under an applied load of 9.8 N (Fig. 4b–d).[245] The gel was prepared by dissolving gelatin in a glycerol solution (40 vol%) and then applying an electric field (20 V cm^{-1}) to produce the physically cross-linked network. It was incubated at 10 °C for 12 h and then immersed in a 2% formaldehyde aqueous solution to produce a chemically cross-linked network in addition to the initial physical network. Since the gel was wet and soft, which made the experiment technically challenging, the authors carefully placed the gels between two electrodes and recorded the piezo signals (Fig. 4c). It is noteworthy to mention that the electric field used in the experiment helped to generate piezoelectricity by inducing polar polypeptide chains as molecular dipoles in the direction of the electric field. The piezoelectricity of gelatin gel is mainly

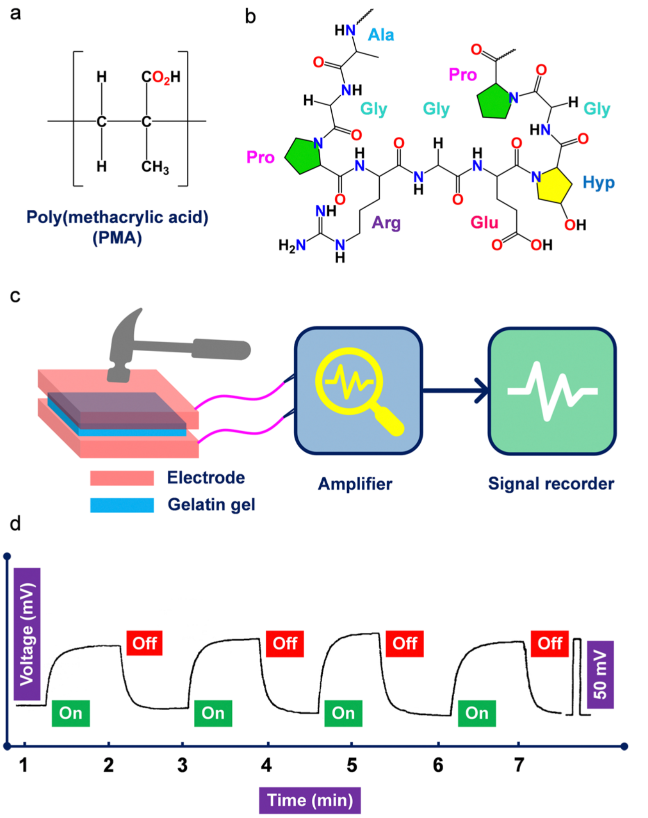

Fig. 4 (a) Chemical structures of poly(methacrylic acid) and (b) gelatin polymers used to develop P-PEGs. (c) Schematic representation showing the instrument used for the piezoelectric measurement of gelatin hydrogel. (d) Piezoelectric output voltage was observed using the gelatin hydrogel device under an applied load of 9.8 N. Reproduced with permission.[245] Copyright © 1996, WILEY-VCH Verlag GmbH & Co. KGaA, Weinheim.

due to directed molecular dipoles, resulting in a piezoelectric output voltage of ~50 mV (Fig. 4d). Moreover, the origin of the piezoelectric polarization and the orientation of the polar polypeptide chains were confirmed by polarized infrared and thermally stimulated current experiments. The authors further stated that the as-prepared gelatin gel was anisotropic. The effect of the electric field assisted in aligning its microscopic dipoles in the direction of the electric field, which was essential to achieving maximal piezoelectric performance. Furthermore, the authors discovered that increasing the crosslinking duration time decreased voltage generation and that increasing the gel ionic strength increased voltage generation, whereas stress of 9.8 N surpassed the electric regimen and voltage remained constant. Other piezoelectric hydrogels, such as gellan gel made of short PVDF and cellulose-neodymium magnet-based magnetoelectric, have attracted significant interest in PEGs energy harvesting application.[174,246]

4.3.2 PVDF-PAN based P-PEGs for sensing applications. Flexible sensors have been extensively studied for the development of healthcare, soft robotics, artificial intelligence, and wearable sensor technologies owing to their superior capability to emulate the characteristics of human skin by integrating a wide range of environmental inputs into electrical signals.[247–249] Since the human skin is a soft, stretchable, water-rich, and breathable biological tissue organ, several known flexible materials have been challenged to replicate it.[250–252] Hydrogels have recently gained significant attention in the domain of artificial skin due to their resemblance to human tissues, since these materials are soft, high-water content, flexible, wearable and show high biocompatibility.[253–255] The majority of hydrogel-based sensors are piezoresistive, based on the principle that the electrical resistivity of a material changes when mechanical strain is applied.[256–258] However, piezoresistive hydrogels show several disadvantages, including an apparent hysteresis effect, low mechanical durability, ease of temperature variations, and the prerequisite for an external source of power, which pose significant barriers to practical application.[259–261] In this context, piezoelectric hydrogels could be a promising alternative solution for self-powered systems, since they do not require any external power supply.[262–265] Recently, Ning and colleagues fabricated a robust and self-powered piezoelectric hydrogel pressure sensor application by dispersing piezoelectric PVDF into a tough PAN matrix (Fig. 5a–k).[266] The PAN-PVDF hydrogel were prepared by copolymerization of PVDF, acrylonitrile, sodium *p*-styrenesulfonate, and methylene-bis-acrylamide crosslinker (Fig. 5a–e). The fabricated piezoelectric PAN-PVDF composite hydrogel displayed a highly electroactive β-phase of PVDF due to the strong dipolar–dipolar interactions between the PVDF and PAN chains.

Given the several polymorphic features of PVDF and the challenges in obtaining a non-centrosymmetric β-phase polar structure for the generation of piezoelectricity, it is plausible that an adequate optimization strategy is required. Moreover, the compressive modulus of the composite 10% PAN-PVDF (30.61 ± 3.97 kPa) hydrogel and 30% PAN-PVDF (96.74 ± 4.73 kPa) hydrogel showed higher mechanical properties compared to pristine PAN hydrogel (7.85 ± 1.73 kPa). The significant enhancement of mechanical properties in the composite gels was attributed to the formation of the dipolar interactions between the difluoromethylene (CF_2) dipole of the PVDF molecule and the cyanide (CN) dipole on the PAN molecule. Additionally, the PAN-PVDF (10%) hydrogel showed a maximum piezoelectric coefficient of d_{33} ~ 30 pC N^{-1} due to its higher concentration of the piezoelectric β-phase. To further confirm the composite gels piezoelectric sensing characteristics, the authors carried out an electro-mechanical experiment. The results showed that when an external mechanical load of 18 N was applied, the composite PAN-PVDF (20%) PiezoGel produced a high output voltage of 30 mV and short-circuit current of 2.8 μA. To fabricate a motion sensor of the proximal interphalangeal joint (PIP), the authors secured the sandwich-like construction on an index finger cover using a 3M scotch adhesive tape. Fig. 5f–h shows the PIP joints bending angle (0° to 90°) as a function of output voltage, demonstrating that the hydrogel sensors output voltage increased as the bending angle increased from 0° to 90°. When the PIP joint was linear, no output voltage signal (0 mV) was produced. However, when the PIP joint was bent 90°, the hydrogel sensor produced an output voltage signal of 30.36 mV, which was ~6 times higher than the voltage produced at a bending angle of 15° (Fig. 5h). Furthermore, the

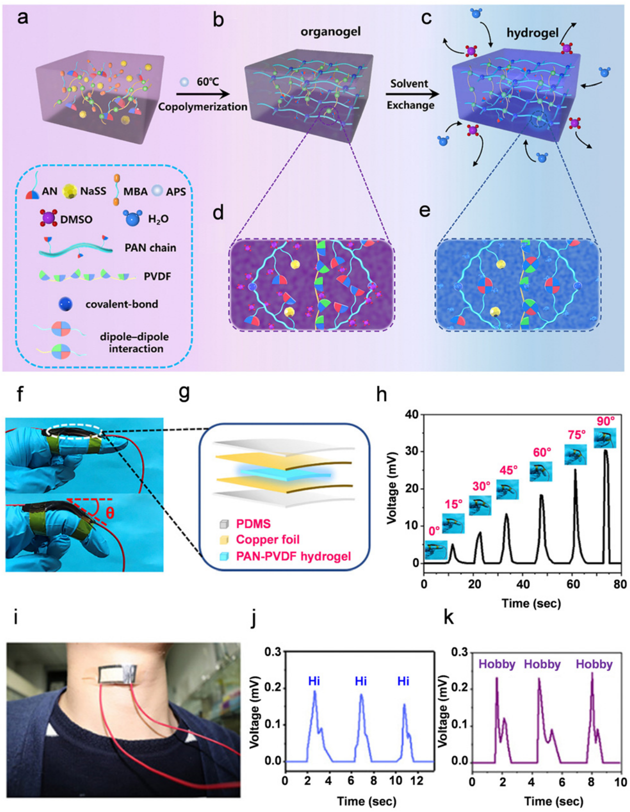

Fig. 5 (a)–(e) Schematic representation of the formation of composite PAN-PVDF hydrogels. Acrylonitrile, AN; sodium *p*-styrenesulfonate, NaSS; methylene-bis-acrylamide, MBA; ammonium persulfate, APS; dimethyl sulfoxide, DMSO; water, H_2O; polyacrylonitrile, PAN; polyvinylidene fluoride, PVDF. (f) and (g) Piezoelectric sensor applications of the PAN-PVDF composite hydrogel showing (f) the optical image of the sensor and (g) schematic diagram of the fabricated piezoelectric PAN-PVDF composite hydrogel. (h) Piezoelectric output voltage was observed from the device by sensing various bending angles (0°–90°). (i) Optical photo of vocal cord vibration detection. (j) and (k) Output voltage signals detection graphs for speaking different words (Hi, hobby, respectively). Reproduced with permission.[266] Copyright © 2019, American Chemical Society.

piezoelectric hydrogel-based pressure sensor served as an artificial skin by recognizing physiological movements such as finger bending, pulse signal, spoken words and vocal cord vibration (Fig. 5i–k). Thus, this research offers a real-time sensing application of piezoelectric hydrogels and may potentially lead to the advancement of self-powered PiezoGels that are similar to human skin, which has significant potential for applications in artificial skin.

Piezoelectric hydrogels with exceptional structural functionality and highly programmable properties have accelerated the development of sensing devices.[147,267–276] Tian and coworkers recently developed a self-powered motion sensor comprised of PHEMA, graphene oxide (GO), and single-walled carbon nanotubes (SWCNTs).[267] The degree of piezoelectricity and sensing properties of the nanocomposite hydrogel was determined by the surface area of the GO and the high strength of the SWCNTs. Piezoelectric polymer gels can also be responsive to various stimuli such as temperature, pH, light, humidity, *etc.* In one instance, Vittorio and coworkers reported PEO-DA-CEA-AlN (diacrylate, DA; 2-carboxyethyl acrylate, CEA)-based flexible mass sensor for the detection of sweat pH.[268] In addition to its exceptional adaptability, the PEO-DA-CEA-AlN sensor detected artificial sweat formulation in pH ranging from 3 to 8. Another intriguing use for polymeric PiezoGel was for object contour recognition. In 2023, Lee and coworkers employed a PVDF-based composite hydrogel tissue-adhesive piezoelectric soft sensor (TPSS) to develop *in vivo* self-powered implantable bioelectric devices for pressure sensing.[269] As a pressure sensor, the TPSS displayed high output voltage of 8.3 V and a high energy power density of 186.9 $\mu W\ m^{-2}$. In addition, the composite hydrogel sensor demonstrated robust adherence to a variety of engineering materials and biological tissues. The contribution by Son and coworkers addressed the exciting prospect of using skin-like transparent polymer-hydrogel (PAM-SA-PVDF-HFP-DBP, sodium-alginate, SA; dibutyl phthalate, DBP) to detect pressure sensing.[270] The developed hybrid sensor displayed dehydrative resistance, transparency, stretchability, and sensitivity desired for flexible and sensing electronics applications. Almost concurrently, the fabrication of piezoelectric polymer gels for the application of human motion sensing was presented by the groups of Chongle Zhao and Yupeng Mao.[271,272] The transparent and soft P-PEGs composed of PVDF, PAM and lithium chloride (LiCl), adhered to the human body due to their bio-compatibility, transparency, and lack of allergic or rejection responses. The P-PEGs were designed to detect a variety of human body movements, including bending, twisting, wrist, elbow, and rotation motions. Other interesting examples of polymeric gel-based PiezoGels were demonstrated for strain, humidity, force, and temperature sensing.[273–275] These polymeric gels, PVDF-polypyrrole-gelatin;[273] p(NVCL-*co*-DEGDVE)-ZnO, (poly-*N*-vinylcaprolactamco-di(ethylene glycol) divinyl ether, p(NVCL-*co*-DEGDVE);[274] PVDF-TrFE-CHACC (chitosan quaternary ammonium salt, CHACC),[275] displayed superior piezoelectric properties and sensing capabilities. In addition to these excellent reports, Wu and coworkers described the metal-ion-induced hierarchical structure and biological tissue-mimicking properties of polymer gels composed of P(AM-AN-MA)-Fe^{3+} (acrylamide, AM; maleic acid, MA; ferric ion (Fe^{3+}).[276] The authors judiciously selected the Fe^{3+} ion to form a hierarchical architecture with copolymerized AM by following a simple salting out and coordination cross-linking strategy. The fabricated PiezoGel displayed several advantages including high water-content (~84%), high tensile strength (1.4 MPa), high toughness (5.1 MJ m^{-3}), low elastic modulus (0.06 MPa), extreme strain-stiffening capability (27.5-fold true modulus enhancement), excellent self-recovery, extremely good durability and tissue-like-mechanical properties. All of these findings offer smart design possibilities and present new ways to expand polymer-based PiezoGels for use in energy harvesting and sensing applications.

4.3.3 PVDF-ZnO-sodium alginate (SA) based P-PEGs for wound healing applications. Recently, Fan and coworkers developed a 3D printed piezoelectric wound dressing based on ZnO nanoparticles (NPs) decorated PVDF-SA dual piezoelectric responsive hydrogel (ZPFSA), which mimics and amplifies bioelectricity to stimulate wound healing and prevent scar

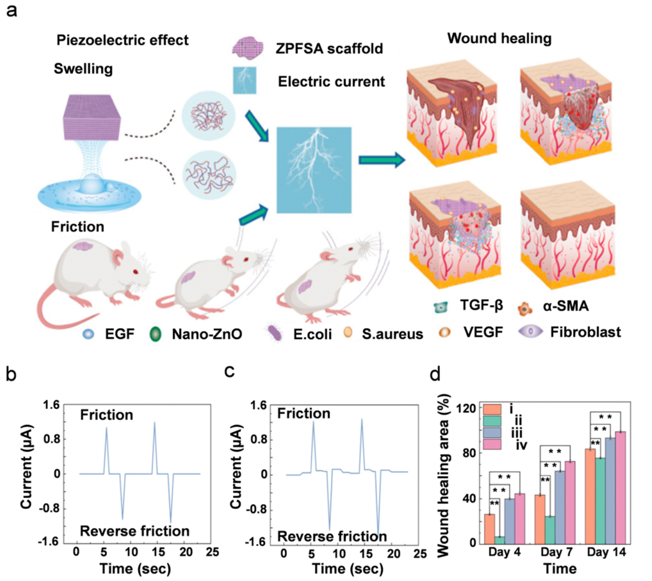

Fig. 6 (a) Schematic representation of 3D printed piezoelectric wound dressing model of ZnO NPs modified PVDF-SA piezoelectric hydrogel scaffold (ZPFSA). (b) and (c) Piezoelectric response of displaying output currents of ZPFSA (0.5) PiezoGel scaffold. (b) Simple frictional action. (c) Frictional action during swelling. (d) Wound healing rate of different piezoelectric scaffolds showing the efficacy of wound healing. (i) control; (ii) SA; (iii) ZPFSA 0; (iv) ZPFSA (0.5), * denotes $p < 0.05$, ** denotes $p < 0.01$. Reproduced with permission.[277] Copyright © 2022, American Chemical Society.

tissue formation (Fig. 6a–d).[277] The dual piezoelectric ZPFSA hydrogel is primarily composed of vertical swelling and horizontal friction models that are utilized to promote wound healing and prevent scar formation. Considering the high hydrophobicity of the PVDF polymer, the authors rationally modified it with ZnO hydrophilic NPs, which exhibit several advantages such as enhanced hydrophilic environment, crystal phase transformation, promoting polarization, excellent antimicrobial activities, and acting as a nucleating agent to enhance the electroactive β-phase of PVDF which is highly desirable for 3D printing and wound dressing applications (Fig. 6a). Moreover, SA has nontoxic, biocompatible, and biodegradable features and reduces the hydrophobicity of PVDF, facilitating the generation of diverse shapes of hydrogels by 3D printing. Further, the dual piezoelectric hydrogel provided bioelectric stimulation and the resultant stress-responsive output current characteristics were monitored by a high-precision benchtop digital multimeter. Fig. 6b and c demonstrate the output current of ZPFSA 0.5 (containing 0.5% ZnO NPs), which produced average values of ±1.10 μA and ±1.29 μA for friction alone and frictional action during swelling, respectively. In both cases, the output current of the ZPFSA 0.5 hydrogel was higher than the SA and ZPFSA 0 scaffolds, indicating the effect of the nano-ZnO concentrations on the polar crystalline phase of PVDF.

Furthermore, the degree of wound healing was tested in Sprague–Dawley rats using a wound defect model at intervals of 4, 7, and 14 days (Fig. 6d). After 7 days, the ZPFSA 0.5 scaffold showed higher wound healing activity than the other scaffolds (control, SA, and ZPFSA) due to the presence of ZnO NPs which improve the antibacterial activity to heal the wounds. Such findings shed light on the importance of piezoelectric scaffolds in stimulating wound healing and extending a new range of applications in the domain of skin wound healing by using PiezoGels as wound dressers.

4.3.4 PVA–PVDF based P-PEGs for wound healing applications. In another innovative work developing PiezoGel for wound healing, Wang and coworkers developed a biocompatible and self-powered piezoelectric composite hydrogel composed of PVA–PVDF, which displayed superior characteristics of mechanical strength, stretchability, cytocompatibility, diabetic wound healing and good piezoelectric response (Fig. 7a–d).[278] The preparation of the PVA–PVDF composite hydrogel involved four distinct stages: freezing/thawing-solvent replacement-annealing-swelling. This unique method gives rise to the crystalline structure and electroactive β-phase in the composite PVA–PVDF hydrogels through hydrogen bonding interactions between the chains of PVA and PVDF. The development of crystalline structures was attributed to the intermolecular interactions of the PVA–PVDF composite gels, which encouraged the PVDFs electroactive β-phase through hydrogen bonding as characterized by Fourier transform infrared (FT-IR) spectroscopy, Raman spectra and powder X-ray diffraction studies. Further, composite PVA–PVDF hydrogels with varying PVDF compositions were examined for their piezoelectric response properties. The output voltage and current were found to be at their maximum values for the 7 : 3 (PVA–PVDF) composite PiezoGel, and the d_{33} was 8.4 pC N^{-1} at an acceleration of 8 m s^{-2}. In addition, in the PVA–PVDF hydrogel, the PVDF phase was evenly distributed all across the PVA matrix generating a compact network assembly with substantial cross-linking density and providing outstanding mechanical robustness and durability in the hydrogel.

Furthermore, owing to their excellent piezoelectric response, the authors investigated the cell culture and cytocompatibility of the PVA–PVDF composite hydrogels. Fig. 7a shows the schematic representation of the formation mechanism of the PVA–PVDF composite PiezoGel and its wound-healing stimulation mechanism in diabetic rats. It was shown that the composite hydrogels support re-epithelialization, collagen deposition, angiogenesis, growth and factor secretion, as well as control macrophage and inflammatory factor levels. Moreover, the efficacy of the PVA–PVDF PiezoGel in wound healing resulted in a progressive change in the wound area. As shown in Fig. 7b, untreated wounds (control) and PVA-treated wounds showed some wound closure after 14 days, but the piezoelectric PVA–PVDF composite hydrogel showed a more significant wound closure, demonstrating the superior healing ability of the latter. Moreover, the PVA–PVDF composite PiezoGel could convert the mechanical energy into electrical energy by the rat's physical activity and the local stimulation generated by piezoelectric hydrogels evenly transferred to the wound bed in real-time. Furthermore, statistical analysis of a hematoxylin and eosin (H and E) staining assay was used to test the width of the granulation tissue and epithelial gap at the tissue level

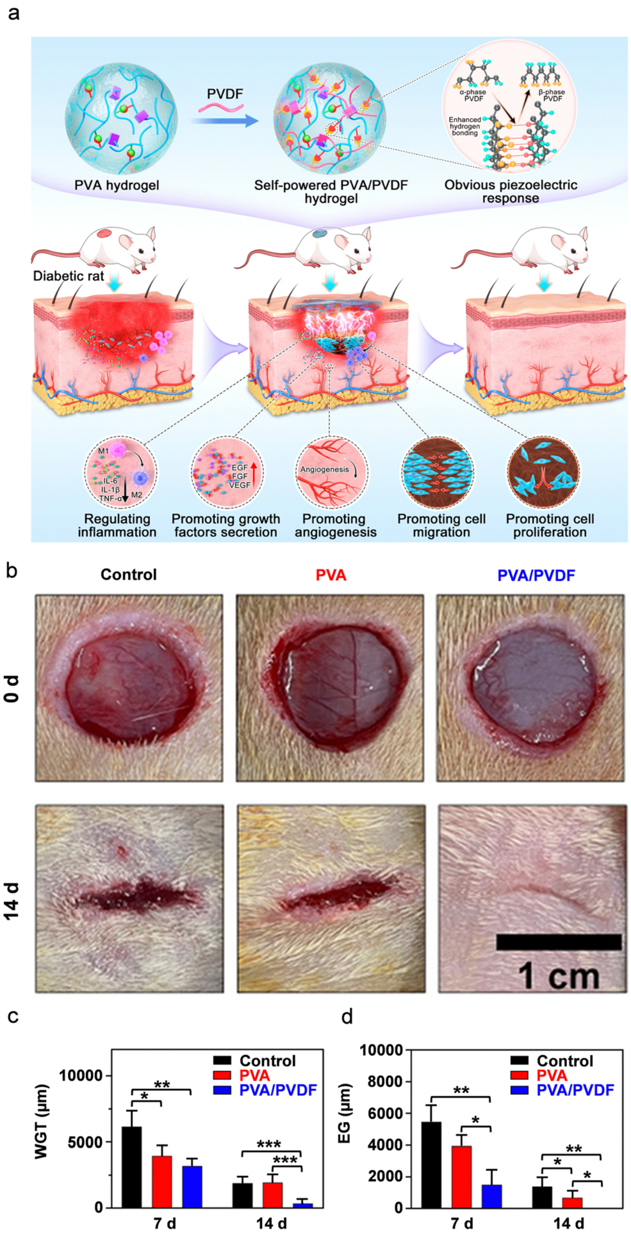

Fig. 7 (a) Schematic representation of the formation mechanism of a PVA/PVDF composite PiezoGel and its wound healing advancement mechanism in diabetic rats. (b) Representative pictures of wounds in diabetic rats treated with control, neat PVA and PVA–PVDF composite PiezoGel at timepoint 0 and after 14 days. (c) and (d) Descriptive statistics of (c) the width of granulation tissue (WGT) and (d) epithelium gap (EG) based on hematoxylin and eosin (H & E) staining assays. Reproduced with permission.[278] Copyright © 2022, American Chemical Society.

(Fig. 7c and d). The results showed that the granulation and epithelium gaps were smaller in the piezoelectric PVA–PVDF hydrogel-treated animals than in the neat PVA hydrogel and the control samples. Consequently, regulation of the proliferation, migration, and production of fibroblasts and vascular endothelial cells by triggering the AKT and ERK1/2 signaling trails to promote wound healing was demonstrated. Such emerging advantages of PiezoGels offer an alternative to conventional electrical stimulation devices and encourage their use in new therapeutic applications such as chronic wound healing, disease diagnosis, and potential bio-clinical treatments.[279–282]

4.3.5 Polyacrylonitrile-acrylamide-styrenesulfate-poly (vinylidene fluoride) (PAAN-PVDF) based P-PEGs for pressure injuries (PIs) or pressure ulcers (PUs) applications. Medical device-related pressure injuries (PIs) are one of the most common adverse events in hospitalized patients worldwide.[283–285] These injuries are typically caused by sustained pressure on the skin resulting in injury to the skin and the underlying tissue. Such injuries cause major distress for hospitalized patients, resulting in prolonged hospital stays, difficulties in healing and pain, higher human suffering, and increased morbidity, and ultimately comprising a significant burden for the global healthcare system.[286–289] Therefore, prophylaxis and management of PIs must be addressed urgently to prevent early prophylactic complications and avoid the need for subsequent treatment. Several dressings were investigated to prevent and manage PIs, including commonly employed polyurethane and hydrocolloid dressings; however, these dressings had drawbacks such as poor conductivity and high rigidity.[290–295] In this context, hydrogel dressings have received a lot of attention for their ability to minimize pressure and maintain a moist environment for the skin to prevent PIs.[296–298] Moreover, hydrogels with piezoelectric properties provide significant advantages due to their outstanding mechanical-to-electrical response, regulation of blood flow, and stimulation of angiogenesis.[299,300] Very recently, Ning and coworkers developed a piezoelectric hydrogel based on PAAN-PVDF for PIs or PUs (Fig. 8a–h).[301] The piezoelectric gels demonstrated outstanding stretchability, skin-like ductility, and significant mechanical properties with Young's modulus values (0.48 ± 0.03 MPa) that match those of human skin (0.5–1.95 MPa). Moreover, the mechanical–electrical properties analysis revealed that the alignment of dipole moment under a certain applied pressure between acrylonitrile and PVDF resulted in the piezoelectric output characteristics. A schematic diagram of dipole moment alignment and the observed output piezoelectric voltage of the piezoelectric hydrogel are shown in Fig. 8a. Piezoelectric energy harvesting of the pristine PAAN hydrogel resulted in an output voltage of 7 mV; however, the addition of PVDF content increased the piezoelectric signals to a maximum output voltage of 50 mV (15%) under mechanical pressure of 40 N (Fig. 8b). Furthermore, increasing the PVDF concentration resulted in a decrease in output voltage (30 mV, 20%) due to the extremely stiff nature of an electroactive PAAN-PVDF PiezoGel. Additionally, the PAAN-PVDF PiezoGel demonstrated excellent cytocompatibility towards L929 cells, as evident by live/dead and anti-Actin staining (Fig. 8c–e). Owing to the excellent mechanical and piezoelectric properties of the 15% PAAN-PVDF hydrogel, it was further employed to study the effect of the electric field-induced *in vitro* angiogenesis on the formation of PIs/PUs. The authors used ultrasonic therapy to study the impact of electrical stimulation on HUVEC angiogenesis using the Matrigel tube formation assay. The absence and presence of tubular structures in pristine PAAN and 15% PAAN-PVDF hydrogels, respectively, showed the enhancement of *in vitro* angiogenesis of HUVECs under ultrasonic sound (Fig. 8f and g).

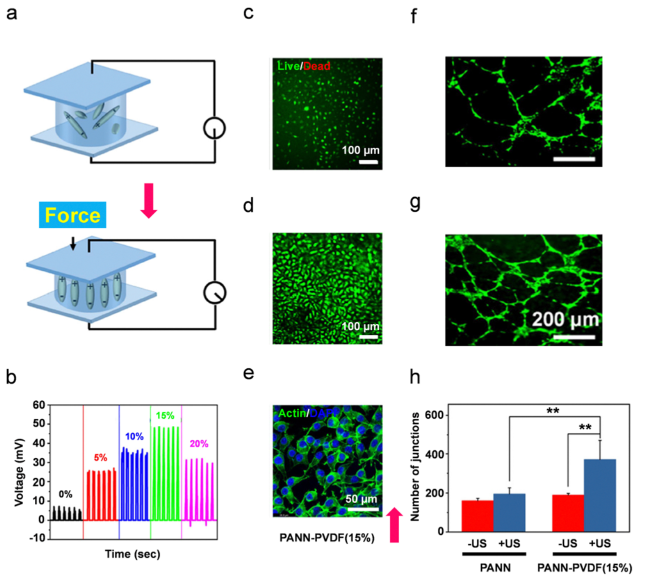

Fig. 8 (a) Schematic representation of polarization alignment under load force application. (b) Piezoelectric output voltage of the PAAN-PVDF hydrogels under an applied mechanical pressure of 40 N. (c)–(e) *In vitro* biocompatibility tests of 15% PAAN-PVDF hydrogels using L929 cells. (c and d) Live/dead staining images. (e) Confocal scanning microscopy images following immunohistochemistry staining using an anti-Actin antibody. (f and g) *In vitro* angiogenesis of human umbilical vein endothelial cells (HUVECs) demonstrating the formation of HUVEC tubular structures after 12 h. (h) The number of junctions of vascular tube formation (*p < 0.05, **p < 0.01,). Reproduced with permission.[301] Copyright © 2022, American Chemical Society.

Furthermore, statistical analysis of the 15% PAAN-PVDF tubes revealed a substantial increase in total length, number of junctions, and meshes compared to PAAN hydrogel (Fig. 8h). Thus, these findings reveal that electrical stimulation of the 15% PAAN-PVDF composite PiezoGel promoted *in vitro* angiogenesis, implying promising applications for early therapy of PIs or Pus Tables 1–3.

4.4 Ceramic oxide-based P-PEGs

Perovskite ceramic oxides are extensively studied families of inorganic piezoelectric materials due to their high-temperature stability, superior mechanical stability, strong resistant structure, high-Curie temperature, and high-piezo- and ferroelectric polarization characteristics. These materials described by the general formula ABX_3, where A is a monovalent cation, B is a divalent metal ion, and X is an oxygen anion.[302–304] In addition, these materials are employed in capacitors, sensors, actuators, detectors, transistors, photovoltaics, storage devices, non-volatile memory devices, and energy harvesters.[305–309] Several materials have been employed in PEG applications, the most prevalent of which are $BaTiO_3$, $PbTiO_3$, $KNbO_3$ and [Pb(Zr, Ti)O_3]. Among these, Pb-based perovskites exhibit a high spontaneous polarization and piezoelectric coefficient and have been extensively explored for a wide range of energy and optoelectronic applications.[310] However, as the demand for human health protection and environmental concern increase, the use of harmful Pb content in electronic devices is strictly restricted, prompting the rapid development of lead-free piezoceramics.[311–315] Although numerous reports on inorganic ceramic oxide-based piezoelectric energy harvesters in the form of the bulk sample, inorganic fillers, and film or polymeric composite materials have been presented,[316–319] hydrogels based on ceramic oxide piezoelectric materials are rarely reported in the literature.

4.4.1 Barium titanate (BTO) NPs containing PVP, PEO based P-PEGs for energy harvesting applications. Recently, there has been increasing interest in the incorporation of piezoelectric ceramic oxides into soft and flexible polymer matrixes as a solution for the brittleness and incompatibility of inorganic ceramic oxides with random mechanical deformations.[320–325] In this context, PVP (commonly known as povidone), a hydrophilic synthetic polymer, has been explored for flexible electronic and biomedical technologies due to its light-weight, flexibility, large specific area, ease of fabrication, solubility, biocompatibility and superior biodegradability.[326–329] Moreover, several studies reported that the PEO is a versatile compound that might be used to prepare hydrogel under mild conditions.[330] Very recently, Frounchi and coworkers reported the piezoelectric behaviour of nanocomposite hydrogels composed of BTO-NPs and a polymeric matrix [typically, PVP and PEO] (Fig. 9a–d).[331] These composite hydrogels were produced utilizing gamma irradiation, which has the advantage of not requiring the addition of any external toxic cross-linkers, initiators, or catalysts. The PVP to PEO ratio and BTO concentration were considered to determine the gel swelling behavior, gel content, viscoelastic behavior, and dielectric and piezoelectric properties.

Moreover, piezoelectric devices with copper electrodes were constructed and their piezoelectric response was investigated by integrating various concentrations of BTO NPs into the polymeric hydrogel networks. Notably, the non-poled PVP-PEO (80 : 20)-3 wt% BTO-NPs device demonstrated no significant output voltage due to the non-piezoelectric cubic phase of BTO. To understand the effects of the poling process and the BTO concentration on the piezoelectric performance, the researchers generated two devices, PVP-PEO (80 : 20)-1 wt% BTO-NPs-35 kGy and PVP-PEO (80 : 20)-3 wt% BTO-NPs-35 kGy, which were pre-poled in an electric field of 1 kV mm^{-1} for 60 minutes. Fig. 9d shows the observed output voltage, with a peak-to-peak output voltage of 100 mV for PVP-PEO (80 : 20)-3 wt% BTO-NPs under a mechanical stimulation of 1 N and applied frequency of 3 Hz. These observations showed that poling and optimal concentration loading of BTO-NPs in PVP-PEO (80 : 20)-3 wt% nanocomposite hydrogels resulted in a stronger piezoelectric response compared to PVP-PEO (80 : 20)-1 wt% BTO-NPs.

4.4.2 Aminated-BTO nanoparticles containing gelatin (Gel), oxychondroitin sulfate (OCS-ABTO)-based P-PEGs for sensing applications. Expanding the applications of hydrogel-based sensors, especially for flexible, stretchable and wearable bioelectronic devices, piezoelectric components have been used to enhance the output performance of the hydrogel sensors. Recent, reports presented the enhancement of hydrogel energy harvesting/sensing performance by the use of piezoelectric

Table 1 Summary of the applications and output performance of polymers-based piezoelectric hydrogel PEGs discussed in Section 4.3

PiezoGel type	Application	Piezoelectric coefficient	Voltage	Current/ current density	Power/ power density	Input/ sensitivity	Area	Ref.
BC-NdFeB	Energy harvesting	—	15 μV	—	—	Periodic force	—	174
Gelatin	Energy harvesting	—	50 mV	—	—	9.8 N	2.5×2.5 cm^2	245
PVDF-glass flake	Energy harvesting	—	~375 mV	—	—	10 ± 2 N, 3 Hz	1×1 cm^2	246
PVDF-PAN	Artificial skin sensing	30 pC N^{-1}	30 mV	2.8 μA	—	18 N	—	266
PHEMA-GO-SWCNTs	Human motion sensing	—	84 mV	—	—	0.94 s^{-1}	—	267
PEO-DA-CEA-AlN	pH-sensing	—	—	—	—	12 kHz pH^{-1}	—	268
TPSS	Pressure sensing	—	8.3 V	1.26 μA	186.9 μW m^{-2}	Bending strain 36.3%	3×1.5 cm^2	269
PAM-SA-PVDF-HFP-DBP	Pressure sensing	—	—	—	—	7.7 Pa^{-1}	—	270
PVDF-PAM-LiCl	Human motion sensing	—	5.41 V	—	—	1 Hz	5×2 cm^2	271
PVDF-PAM-LiCl	Human motion sensing	—	3.96 V	—	~1 μW	15 N	—	272
PVDF-polypyrrole-gelatin	Strain sensing	13 pC N^{-1}	—	—	—	32.39 kPa^{-1}	1×1 cm^2	273
p(NVCL-*co*-DEGDVE)-ZnO	Humidity and human motion sensing	20 pC N^{-1}	—	0.21± 0.02 nA	—	4–20 N, 364 ± 66 pC N^{-1}	1×1 cm^2	274
PVDF-TrFE-CHACC	Strain sensing	5.3 pC N^{-1}	100 mV	0.12 μA	—	5–25 Hz	—	275
P(AM-AN-MA)-Fe^{3+}	Pressure sensing	—	~0.27 mV	—	—	0.094 mV kPa^{-1}	—	276
PVDF-ZnO-SA	Wound healing-rat skin	—	~200 mV	±0.386 μA	—	—	1×1 cm^2	277
PVA–PVDF	Diabetic wound healing-rat's body	8.4 pC N^{-1}	2.82 V	248.16 nA	—	8 m s^{-2}	500 μm	278
Aligned PVDF nanofiber	Wound healing	—	0.85 V	40 nA	—	6.5 N, 1 Hz	1×1 cm^2	279
PVDF-CS-gelatin-PVA	Wound healing	—	~80 mV	—	—	—	5×8 cm^2	280
BM-CMCS-TA-FWO	Wound healing	—	—	—	—	—	—	281
PVA–PVDF-Ag-HA	Osteochondral defect repair-rabbit's cartilage area	—	0.36 V	—	—	—	—	282
PAAN-PVDF	Energy harvesting/pressure injuries	—	50 mV	—	—	40 N, 0.5 Hz	—	301

Table 2 Summary of applications and the output performance of perovskite ceramic oxides piezoelectric hydrogels-based PEGs discussed in Section 4.4

PiezoGel type	Application	Piezoelectric coefficient	Voltage	Current/ current density	Power/ power density	Input/Sensitivity	Area	Ref.
$BaTiO_3$-PVP-PEO	Energy harvesting	—	100 mV	—	—	1 N, 3 Hz	—	331
Gel-OCS-ABTO	Sensing	—	85–90 mV	—	—	0.64–12.74 kPa	0.8 cm (t), 1 cm (D)	333
PEGDA-AuBTO-GelMA	Wound healing	—	—	—	—	—	—	336

Table 3 Summary of applications and the output performance of supramolecular piezoelectric hydrogel–based PEGs discussed in Section 4.5

PiezoGel type	Application	Piezoelectric coefficient	Voltage	Current/ current density	Power/ power density	Input/sensitivity	Area	Ref.
DH-PUU	Energy harvesting/ human–motion sensing	62 pC N^{-1}	2.5 V	1900 nA	1.7 mW m^{-2}	25.5 kPa, 6 Hz	—	356
Im-ClO_4-BC	Keyboard sensing	46 pC N^{-1} (Im-ClO_4)	140 mV	—	—	31.25 kPa, 4.24 mV kPa^{-1}	2×2 cm^2	357
Fmoc-FF	Energy harvesting	1.7 ± 0.5 pm V^{-1}	—	—	—	12 nN, 12.5 kHz	—	376

materials such as inorganic ceramic oxides.[71,332] In one such example, Ning and coworkers described a multichannel wireless sensor system based on a Gel-OCS-ABTO composite hydrogel, which demonstrated superior electrical performance along with exceptional flexibility, stretchability, and biocompatibility (Fig. 10a–g).[333] The Gel-OCS-ABTO composite PiezoGel was prepared in PBS buffer by dissolving Gel, lyophilized boronate-diol complexation of CS and the incorporation of aminated-BTO nanoparticle at different concentrations (0, 1%, 3%, and 5%). It is interesting to note that all Gel-OCS-ABTO hydrogels could be elongated multiple times, especially the Gel-OCS-ABTO (3%) composite hydrogel, which could be elongated more than 200% (largest elongation, 225%) without breaking (Fig. 10a). The tensile strength of the hydrogels was also enhanced by the addition of BTO and it was observed that Gel-OCS-ABTO (5%) had a maximum Young's modulus of 220 kPa, indicating the dominant effect of the concentration of inorganic particles on the tensile Young's modulus. The composite gels showed remarkable biocompatibility due to the natural origin of Gel and CS, as well as the biocompatibility of BTO (Fig. 10b).

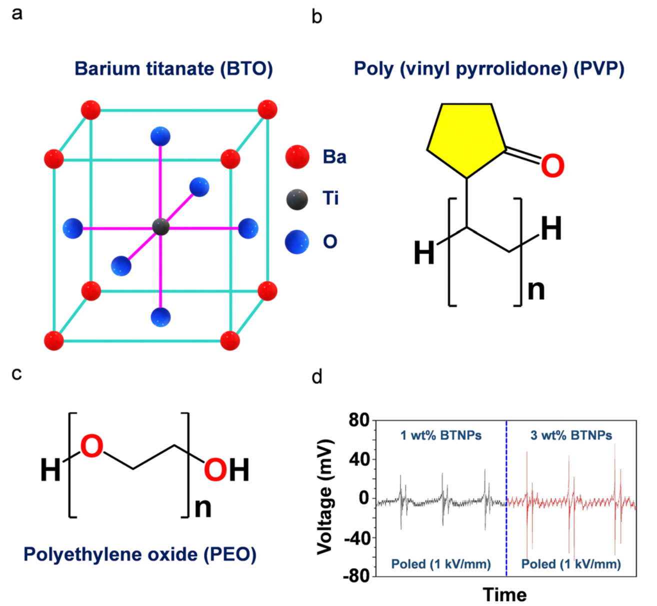

Fig. 9 (a)–(c) Schematic structures of (a) BTO, (b) PVP, and (c) PEO. (d) Piezoelectric output voltage of poled PVP-PEO (80 : 20)-(15 wt%) (left) and PVP-PEO (80 : 20)-(15 wt%) (right) containing 1 wt% and 3 wt% of BTO-NPs. The experimental parameters used in this study were 1 N, 3 Hz, and 1 sec of mechanical stimulation, applied frequency, and time, respectively. Reproduced with permission.[331] Copyright © 2022, Elsevier Ltd.

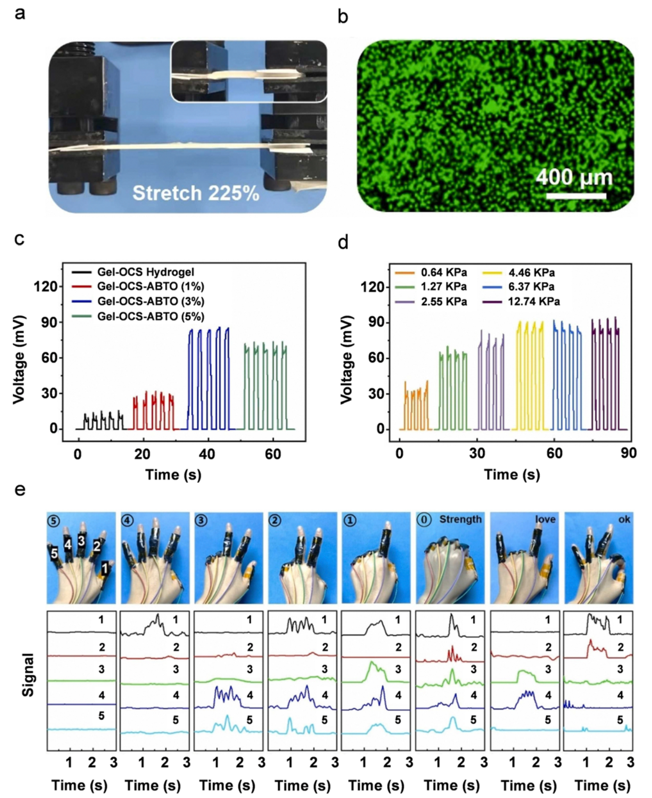

Fig. 10 (a) Schematic illustration of stretchable and biocompatible Gel-OCS-ABTO composite hydrogels. (b) and (c) Piezoelectric energy harvesting performance of (b) output voltage as a function of different ABTO concentration under a constant stress of 4.46 kPa and (c) output voltage as a function of different applied stress levels. (e) Photographic images and piezoelectric signals of the Gel-OCS-ABTO hydrogel under different finger gesture operations. Reproduced with permission.[333] Copyright © 2023, Elsevier Ltd.

A mechanoelectrical experiment using Gel-OCS-ABTO at different ABTO concentrations was carried out under a constant stress of 4.46 kPa. The results showed a maximum output voltage of 85–90 mV for Gel-OCS-ABTO (3%) demonstrating the homogeneous distribution of ABTO nanoparticles (Fig. 10c). Moreover, the output voltage signals of the Gel-OCS-ABTO (3%) sensor under different stress levels revealed that the output voltage significantly increased with increasing stress up to 4.46 kPa.

The growth trend of the output voltage tended to be flat, which meant that as the stress increased to 12.74 kPa, the output voltage only increased from 90 mV to 94 mV (Fig. 10d). As a pressure sensor, the piezoelectric device showed real-time wirelessly monitoring of physiological signals such as human gesture recognition, knee flexion, elbow flexion, plantar pressure distribution and precise signal detection performance in real-time without any external power source (Fig. 10e). This work represents a significant advancement in the field of PiezoGel-based wireless multichannel sensing systems by illustrating the potential for e-skin, health monitoring, and implanted bioelectronics applications.

4.4.3 BTO-decorated and 3D-printed Janus piezoelectric composite hydrogels-based P-PEGs for wound healing applications. Wound healing and preventing wound infection have become a major challenging problem and represent a considerable public healthcare burden.[334,335] Even though these two processes are closely related, they seldom co-occur in the natural state, which slows down the healing of wounds. Numerous wound dressings have been reported over the years, however, they often lack structural design and regulated payload release, rendering them unable to meet the variety of needs in various wound healing processes. To address this issue, new wound dressings with distinct architectures and controlled release of drug characteristics are needed. Recently, Zhao and coworkers developed a 3D-printed Janus PiezoGel using a poly(ethylene glycol) diacrylate (PEGDA) hydrogel with gold-nanoparticle-decorated barium titanate (Au-BTO) as the top layer and methacrylate gelatin (GelMA) as the bottom layer for programmable antibacterial wound healing (Fig. 11a–f).[336] In this study, the authors stated that the use of the top Au-BTO layer could facilitate the controlled release of the ultrasound (US)-triggered piezocatalytic reactive oxygen species (ROS) while preventing nanomaterial leakage. Notably, the internal bioactivity of the bottom GelMA hydrogel layer along with the steady release of vascular endothelial growth factor (VEGF) promoted cell proliferation and tissue regeneration. Most importantly, the biodegradability of the GelMA hydrogel ensured the avoidance of removal patches at the wound site (Fig. 11a).

The BTO-composite piezoelectric Janus hydrogel patches were prepared using a simple extrusion-based 3D-printer and a layer-by-layer scalable fabrication method. The bottom layer was printed first, followed by the top layer, and both layers were continuously exposed to ultraviolet (UV) light. To maintain the bio-ink shape and consistency during printing, a high concentration of alginate was used. Further, the PiezoGel patches were

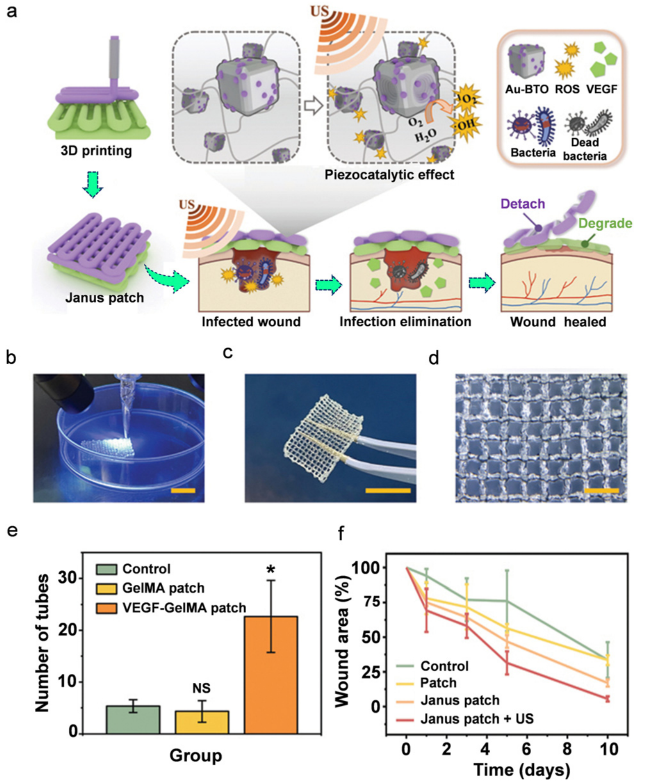

Fig. 11 (a) Schematic illustration of the fabrication and application of the piezoelectric hydrogel patch for wound healing. (b)–(d) Real-time imaging of (b) the UV-assisted 3D printing, (c) digital, and (d) optical images of the 3D-printed PiezoGel patch. (e) Statistical analysis of the number of capillary-like structures of HUVECs cultured in VEGF-patch. (f) The relative wound area curve from day 0 to day 10. Reproduced with permission.[336] Copyright © 2023, American Association for the Advancement of Science.

immersed in calcium chloride ($CaCl_2$) solution, which ionically crosslinks with Ca^{2+} *via* alginate, enhancing the mechanical strength and durability of the hydrogel patches. The real-time 3D printing process is shown in Fig. 11b, illustrating the hydrogel patches good printability and shape consistency. As shown in Fig. 11c and d, the PiezoGel patch displayed superior mechanical durability and robust mesh-designed structures. Further, periodic ultrasonic vibration was used to confirm the mechanical deformation and piezoelectricity of the tetragonal BTO. Upon the separation of the electron–hole pairs on the BTO, a built-in electric field was created, which resulted in the redox processes that produce ROS. In addition to piezocatalytic effects, the US-excited PEGDA hydrogel patch encapsulated in Au-BTO (Au-BTO@patch) was used to demonstrate antibacterial activity against Gram-positive (*Staphylococcus aureus*) and negative (*Escherichia coli*) bacteria.

Furthermore, the authors studied the influence of a VEGF-loaded GelMA patch (VEGF-patch) on tissue engineering and wound healing. In general, it is anticipated that VEGFs will act as potent mitogens, encouraging the migration of endothelial cells and the development of blood vessels. In order to examine the proangiogenesis function of the VEGF-patch, the authors selected HUVECs to perform the tube formation study. As seen in Fig. 11e, a small number of capillary-like structures were formed by HUVECs cultured in both a blank medium (control group) and a medium containing an unloaded GelMA hydrogel patch (GelMA patch group). In contrast, the VEGF-patch-cultured HUVECs displayed a significant number of tube structures. Remarkably, it was shown that the GelMA-encapsulated VEGFs maintained outstanding bioactivity even after the 3D-printing process and were released from the GelMA hydrogel fibers, indicating a simple fabrication process and the biofriendliness of GelMA.

Encouraged by these excellent *in vitro* results, the authors performed *in vivo* experiments to evaluate the antibacterial efficacy and proangiogenesis activity of the 3D-printed PiezoGel patch. Full-thickness wounds 1 cm in diameter were inflicted to the back skin of Sprague–Dawley rats. The rats were divided into 4 groups at random: control, the empty-loaded gauze group, the Janus patch group, and the Janus patch + US group (Fig. 11d). The wound area of all the groups decreased from 0 to day 10. The wounds in the Janus patch + US group demonstrated the best results when compared to the other three groups (Fig. 11d). The results showed fast infection elimination and antimicrobial activity of the Janus patch + US group, which promoted faster wound healing. Such 3D-printed PiezoGels-based PEGs sensors with practical significance in sonodynamic treatments and the development of intelligent patches for improving wound healing are expected to be more widely employed in the future.

4.5 Supramolecular materials-based P-PEGs

Supramolecular piezoelectric materials-based hydrogels are organic and hybrid organic–inorganic molecular unit assemblies that can comprise lower dimensional discrete entities or extended networks.[337–340] These materials exhibit significant advantages compared to conventional PiezoGels owing to their facile synthesis, lightweight nature, structural functionality, softability, tunability, adaptability, mechanical flexibility and ease of fabrication. One of the key benefits of supramolecular PiezoGels is the propensity to combine multiple structural functionalities *via* numerous non-covalent interactions such as hydrogen bonding, van der Waals, electrostatic, stacking, ionic, and hydrophobic interactions.[341–346] A remarkable combination of mechanical flexibility and multifunctionality is expected to expand the utilization of PiezoGels in biomedical devices and smart power generation, which are currently at the forefront of supramolecular gel chemistry.[347–350] In this section, we highlight the piezoelectric properties observed for supramolecular organic PiezoGel materials comprised of imidazolium perchlorate and fluorenylmethoxycarbonyl (Fmoc)-diphenylalanine (Fmoc-FF). We searched for PiezoGels based on typical metal-containing organic–inorganic hybrid piezoelectric materials, but to the best of our knowledge, no reports presenting such materials are currently available. The hybrid PiezoGels, which can combine both organic and inorganic hybrid counterparts in a single crystalline phase, could be ideal candidates for future research directions aimed at establishing novel ways for catalysis, multiferroics, and bio-electronics systems.[351–353]

4.5.1 Ferroelectric 1,4-diazabicyclo[2.2.2]octane perrhenate (dabcoHReO$_4$, DH)-poly(urethane-urea) (PUU) based P-PEGs for energy harvesting/sensing applications. Flexible electronic skins with piezoelectric energy harvesting characteristics are ideal for implanted electronics that can monitor physiological signals and harness biomechanical energies. Many known piezoelectric materials are stiff and crystalline in nature, apart from a few well-studied polymeric materials such as nylon, PVDF, and its copolymers. As a result, the development of highly flexible and stretchable piezoelectric devices for electronic skin applications with high sensitivity remains a challenge.[354,355] Recently, Hu and coworkers have demonstrated highly stretchable and resilient piezoelectric hydrogel-based sensors made of molecular ferroelectric 1,4-diazabicyclo[2.2.2]octane perrhenate (dabcoHReO$_4$, DH)-PEO-based poly(urethane-urea) (PUU) (Fig. 12a–i).[356] The authors were intrigued to assemble PiezoGels based on molecular ferroelectric DH owing to its simple solution processability, fastest polarization switching, high Curie temperature, and superior piezo- and ferroelectric properties. In addition, DH crystallizes in the acentric monoclinic space group *Cm*, revealing a unique hydrogen bonding association of NH···N bistable linkages that are organized in a directional and parallel pattern (Fig. 12b and c). The networks formed by hydrogen bonding interactions between the hydrophobic segments of PUU and the hydrophilic segments of PEO functioned as water-swellable supramolecular gels that absorbed the aqueous solution of piezoelectric DH.

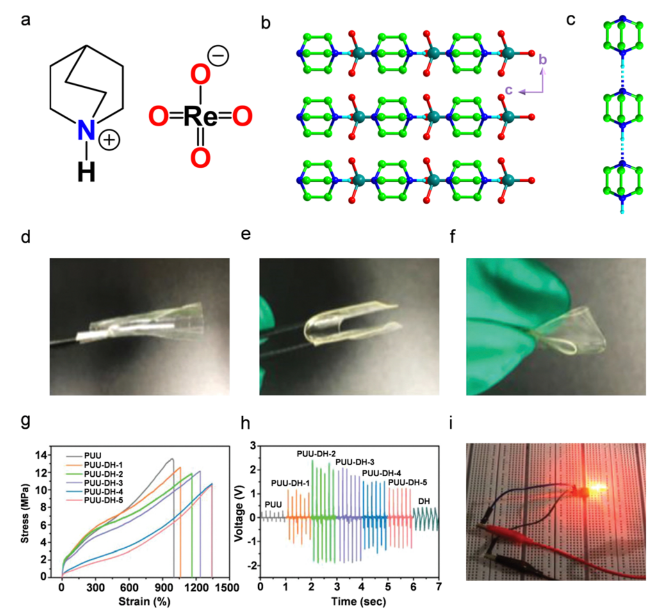

Fig. 12 (a) Molecular structure and (b) crystal-packing higher-order structures of DH are depicted along the crystallographic (100) plane. (c) Representation of dabco cations illustrates parallel bistable hydrogen-bonded interactions mediated by NH···N bonds. To allow structural clarity, the anions ReO_4^- were removed. (d)–(f) PUU-DH-2 optical images showing various deformations. (g) Stress–strain curves of pristine PUU gel and PUU-DH piezoelectric gel composites. (h) Piezoelectric output voltages of neat PUU and PUU-DH composite gels by applying a mechanical pressure and frequency of 25.5 kPa and 6 Hz, respectively. (i) Piezoelectric composite gel (PUU-DH-2) providing power for LED light-up *via* finger tapping. Reproduced with permission.[356] Copyright © 2021, WILEY-VCH Verlag GmbH & Co. KGaA, Weinheim.

Furthermore, strong hydrogen bonding interactions between the DH and the PEO components in the supramolecular gels resulted in the formation of uniformly dispersed and 3D polymer networks. To tailor the effective electrical and mechanical properties, the PiezoGels were designed with various mass fractions (PUU-DH-1, 3 wt%; PUU-DH-2, 5 wt%; PUU-DH-3, 7.5 wt%; PUU-DH-4, 10 wt%; and PUU-DH-5, 15 wt%;) of DH in the polymeric composites. Fig. 12d–f shows how the fabricated composite gels can be easily deformed by adopting different modes of operation, revealing the exceptional flexibility and stretchability of the piezoelectric PUU-DH composite hydrogel. Moreover, the PUU-DH composite gels exhibited exceptional mechanical properties such as high elongation at break (>1000%), tensile modulus (>2 MPa), toughness (>57 MJ cm^{-3}) and breaking strength (>10 MPa) (Fig. 12g). In addition, the composite PiezoGel revealed superior piezoelectric properties (d_{33} ~ 62 pC N^{-1}), indicating that the fabricated piezoelectric gels can be useful in mechanical deformations and mechanical energy harvesting. Fig. 12h displays the piezoelectric energy harvesting performance of the pristine PUU, pristine DH, and composite gels prepared at various weight percentages under a load pressure of 25.5 kPa and an operating frequency of 6 Hz. The output voltages of both PUU and DH were rather modest, while the output voltages of PUU and DH increased with the DH mass fraction and eventually dropped in the composite gels, demonstrating effective intermolecular interactions between PUU and DH in the composite gels. The 10 wt% (PUU-DH-2) composite piezoelectric gel produced a highest output voltage of 2.5 V (Fig. 12h). Thus, these findings show that the compatibility between the polymeric matrix and the suitable mass fraction of the piezoelectric fillers is a key factor in determining the high electromechanical response of the piezoelectric gels. Moreover, the high piezoelectric performance of the PUU-DH-2 device further demonstrated potential applications of lighting up three LEDs (Fig. 12i). The authors also explored the potential applications in wearable technology and artificial electronic skin by attaching the PUU-DH-2 device to a balloon and human body parts. The results revealed that the device could withstand greater deformation due to the strong mechanical properties of the gel. The results pave the way to designing tough and stretchable piezoelectric gels with promising prospects for use in the development of artificial electronic skin.

4.5.2 Hybrid imidazolium perchlorate (Im-ClO$_4$)-BC based P-PEGs for sensing applications. Recently, Zhang and coworkers reported PiezoGel-based sensors comprised of ferroelectric imidazolium perchlorate (Im-ClO$_4$) and BC, which exhibit remarkable biodegradability and recyclability, highlighting the importance of advancing electronic waste (e-waste)-free materials for the development of sustainable and eco-friendly energy technologies (Fig. 13a–d).[357] The authors judiciously selected the molecular piezo- and ferroelectric component Im-ClO$_4$ due to the easy solution processability, structural flexibility, facile fabrication, superior electromechanical coupling and high piezoelectric coefficient (46 pC N^{-1}) and ferroelectric

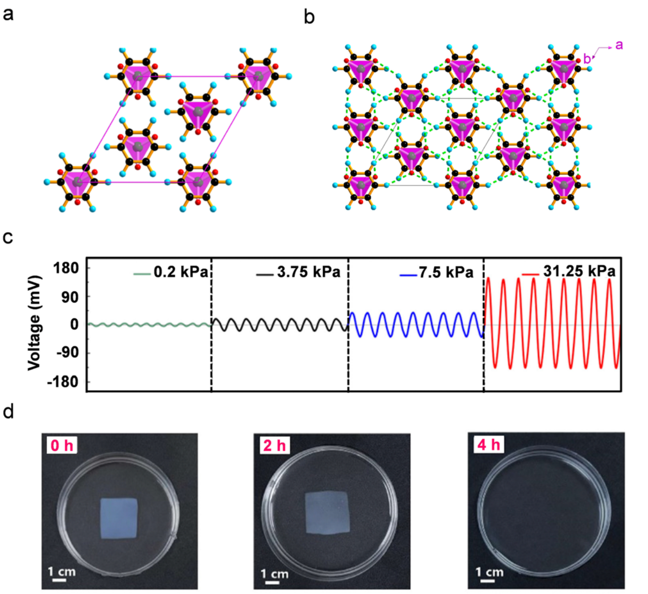

Fig. 13 (a) Crystal packing diagram and (b) formation of three-dimensional higher-order structures *via* hydrogen-bonded interactions of Im-ClO_4. The ClO_4^- anion shows ordered structures with four oxygen atoms occupying four vortexes of the tetrahedron, resulting in the loss of the inversion center. (c) The piezoelectric output voltage of the hybrid sensor under diverse out-of-plane mechanical pressures of 0.2, 3.75, 7.5, and 31.25 kPa. (d) Photographs of BC membrane displaying the degradation process under various time intervals. The BC membrane is completely degraded within four hours in a cellulase solution. Reproduced with permission.[357] Copyright © 2019, American Chemical Society.

polarization (7.5 μC cm^{-2}), characteristics that outperform most of the well-known conventional piezo and ferroelectric materials composed of piezopolymers and piezoceramic oxides.

The single-crystal X-ray diffraction analysis of the Im-ClO_4 unit-cell packing and higher-order crystallographic diagram showed the Im-ClO_4 to be polar and non-centrosymmetric (Fig. 13a and b). The BC hydrogels were produced by the microorganism *Gluconacetobacter xylinus* and characterized using X-ray diffraction, Raman spectra, and FTIR. Furthermore, molecular ferroelectric Im-ClO_4-BC hybrid sensors were produced by immersing the BC hydrogel matrix in an Im-ClO_4 solution which crystallized both organic imidazolium cation and inorganic perchlorate ions between the BC hydrogel layers. The flexible Im-ClO_4-BC hybrid device displayed sensing capabilities towards external mechanical pressure ranging from 0.2 kPa to 31.25 kPa (Fig. 13c). The observed output voltage increased linearly with the applied mechanical pressure, showing a maximum output voltage of 140 mV for 31.25 kPa. Such a wide range of sensitivity outperforms many of the previously-reported biodegradable sensors.

Furthermore, this Im-ClO_4-BC hybrid gel showed outstanding biodegradability and recyclability capabilities. When this hybrid device was immersed in water, both the organic cation and perchlorate ions were completely dissolved. Then, the BC membrane was immersed in cellulase solution and the degradation process was evaluated at different time intervals (Fig. 13d). After four hours, the entire BC membrane had degraded, indicating the outstanding biodegradability of the BC matrix. Interestingly, when compared to the original hybrid Im-ClO_4-BC gel, the recycled imidazolinium perchlorate and BC membrane exhibited no difference. Such an eco-friendly hybrid material provides a new paradigm for the construction of flexible biosensors that are clean of environmental damage and e-waste.

4.5.3 Fiborus peptide Fmoc-FF based P-PEGs for energy harvesting applications. Next-generation electronics must contain bio-supramolecular piezoelectric materials to realize the great potential of mimicking the structural characteristics and functional properties of naturally occurring piezoelectric systems. The impact of bio-supramolecular piezoelectric materials has been explored for diverse applications ranging from energy harvesting to sensing, catalysis, therapy, and biological signaling devices to advance healthcare systems.[358–360] Over the years, amino acid and peptide-based piezoelectric materials were explored owing to their intrinsic chirality, excellent flexibility, high piezoelectricity, strong hierarchical self-assembly behavior, bio-safety, bio-compatibility and bio-degradability.[361–364] So far, powder crystallites, single crystals, and composite materials based on amino acids and short peptides have been tested for energy harvesters or sensor applications. However, excluding a few cases, most examples displayed rigid and complex device architectures that limit their use in flexible and wearable self-powered electronics applications.[365–371] PiezoGels based on amino acids or short peptides could be able to solve these challenges due to their excellent merits of transparency, softness, tissue adherence, excellent mechanical properties and the added benefit of working at low mechanical pressure, such as human-body movements. One of the most studied short aromatic dipeptides is Fmoc-FF due to its ability to form various self-assembled ordered nanostructures (*i.e.*, nanotubes, nanorods, nanospheres, nanocylinders,

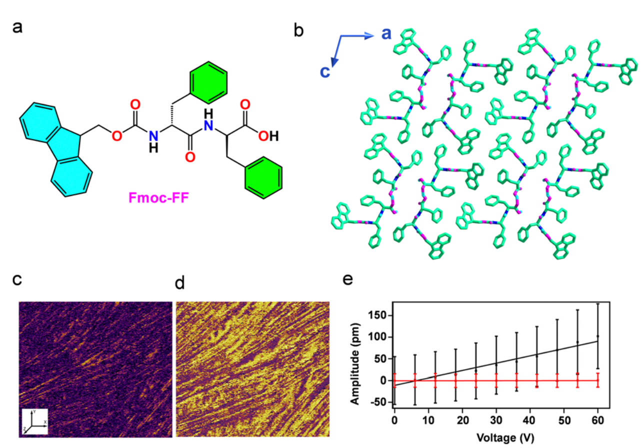

Fig. 14 (a) Chemical structure of Fmoc-FF and (b) higher-order crystal packing diagram showing β-sheet hydrogen-bonded structures packed along the crystallographic 'b' axis (CCDC: 1027570).[377] (c) and (d) Lateral piezoresponse force microscopy (L-PFM) analysis showing (c) amplitude and (d) phase images. (e) Representation of L-PFM amplitude curve as a function of the applied voltage. The slopes are the average local piezoelectric coefficient and piezoresponse signal for a nonpiezoelectric glass slide (red). Reproduced with permission.[376] Copyright © 2015, American Chemical Society.

nanofibers, nanofibrils, *etc.*).[372–375] Rodriguez and colleagues have recently observed piezoelectricity in nanofibrous Fmoc-FF networks using lateral piezoresponse force microscopy (L-PFM) (Fig. 14a–e).[376] Spontaneous self-assembly of Fmoc-FF was proven to give rise to three-dimensional networks with ordered crystalline structures *via* diverse non-covalent interactions that underlined the piezoelectric potential of Fmoc-FF. Single-crystal analysis revealed that Fmoc-FF assembled in the non-centrosymmetric polar monoclinic *C2* space group.[377] Fig. 14b demonstrates higher-order crystal packing networks generated through hydrogen bonding (dotted lines) and rigid aromatic–aromatic stacking along the crystallographic b-axis, resembling unprotected FF piezoelectric nanotubes.[363,378] These structural similarities between Fmoc-FF and FF suggest that Fmoc-FF fibrous networks could exhibit piezoelectricity. The Fmoc-FF PiezoGel was prepared using a typical solvent-switch method, dried, and employed for a piezoelectric experiment. Fig. 14c–e illustrates the L-PFM amplitude and phase images of Fmoc-FF dried gel, revealing the moderate piezoelectric response and inverted phase signals in some regions.

Furthermore, the amplitude vs voltage graph demonstrates the linear dependence as a function of applied voltage, with a shear piezoelectric coefficient (d_{15}) of 1.7 ± 0.5 pm V^{-1} as derived from the slope of the graph (Fig. 14e). The observed piezoelectric response of Fmoc-FF nanofibrils could be attributed to the acentric structure arrangement of the underlying β-sheet topology. This work provides an attractive paradigm for the development and application of many additional piezoelectric biological gels based on amino acids or short peptides.

5. Summary and future perspectives

Flexible electronics derived from renewable energy sources has drawn the attention of the scientific community due to the development of sustainable materials, self-powered systems, and environmental protection, as well as the demonstration of fascinating applications and new opportunities in energy and bio-medicine. This review mainly highlighted new emerging domains of PiezoGels based on polymers, ceramic oxides, and supramolecular materials in the context of energy harvesting, sensing, and wound dressing or healing applications. Unarguably, these PiezoGels have outstanding features such as flexibility, elasticity, wearability, and even eco-friendliness, biocompatibility, and biodegradability, making them an innovative alternative to typical non-flexible devices such as batteries and supercapacitors. In most cases, the developed P-PEGs were capable of powering small electronics by utilizing biomechanical movements and were employed for bio-medical applications such as wound healing, prophylaxis prevention, and pressure injuries/pressure ulcers. Despite the emergence of PiezoGels, several challenges need to be addressed before they can be employed in practical applications such as energy, electronics, and biomedicine. It is important to emphasize that this growing field is currently facing not only great challenges but also intriguing opportunities. The following figures of merit are some of the particularly important considerations for advancing the growth of P-PEGs for use in healthcare, flexible and wearable electronics (Fig. 15).

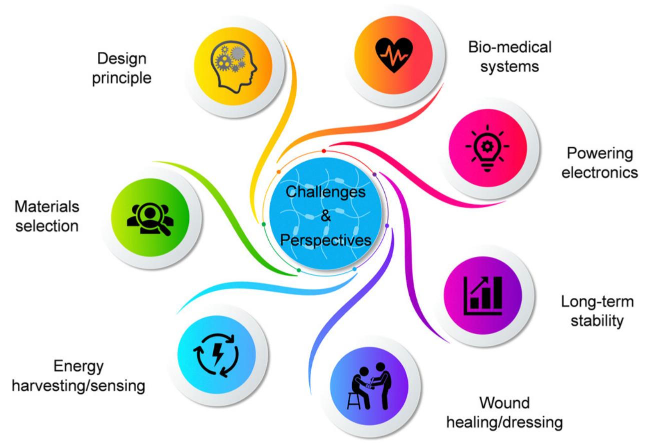

Fig. 15 Challenges and future perspectives of P-PEGs.

5.1 Design principle

The design principle of piezoelectric hydrogels based on PEGs is important to achieving higher output performance for certain applications. At this stage of design, it is important to take into account the various specifications and operational circumstances of the potential application of the hydrogel-based piezoelectric generators. Therefore, when designing P-PEGs, it is important to consider the requisite selection of the appropriate piezo-material, electric power, device architecture, working times, and environmental conditions such as relative humidity, temperature, pressure, and vibrations. It is also important to consider the environmentally sustainable properties, biocompatibility and biodegradability, as these qualities are better suited for PEG applications for energy harvesting, sensing, and other bio-medical applications. One can also examine other specifics of analytical system design and theoretical modeling (such as density functional theory, COMSOL Multiphysics and ANSYS simulations) that may be employed in the design of piezoelectric hydrogel-based devices to find the best working principle, selection of materials, and electromechanical configuration that ensures the biosafety and dependability of the P-PEGs under a variety of working conditions.[379,380]

5.2 Materials selection

The majority of studies on piezoelectric hydrogels has been devoted to examining and enhancing the materials physical characteristics, including transparency, flexibility, stretchability, and mechanical properties. So far, limited attention has been devoted to chemical functional modification aiming to modify the piezoelectric properties as well as their synergy with the output device performance. Therefore, identifying the appropriate material for P-PEG applications is crucial for improving their performance and reliability in various electromechanical applications. For example, many piezoelectric hydrogels were developed based on piezopolymers and perovskite ceramic oxide materials due to their exceptional piezo- and ferroelectric response. Often composed of toxic lead-based systems or other heavy metals, these ceramic materials are brittle, show high stiffness and high density, and require high voltage poling and high-temperature sintering processes, thus limiting their use in wearable electronic applications. Therefore, there is a genuine unmet need for a new generation of high-performance and eco-friendly piezoelectric materials for bio-piezo electronics applications. Moving forward to design bio-compatible and biodegradable piezoelectric hydrogels, supramolecular piezoelectric materials based on amino acid- and/or peptide-containing hydrogels could be an exciting alternative to the traditional materials owing to their light weight, flexibility, bio-safety, bio-degradability, high mechanical strength and high piezoelectric properties. We believe such an innovative direction would pave the way for designing high-performance bio-compatible piezoelectric hydrogel materials for applications in energy and healthcare systems.

5.3 Energy harvesting/sensing

For a self-powered energy harvesting/sensing system to function continuously and reliably, the power density of the energy sources is a critical factor. Currently, the output energy harvesting/sensing performance of P-PEGs is often lower than that of other flexible PEGs. Developing high-performance energy harvesting/sensing P-PEG-based devices is a promising research challenge. Many important considerations, including the optimal choice of high piezo-material, creation of a high surface charge density, robust structural rigidity, and compatibility matching between the piezo-material and polymers, can enhance the output characteristics. However, most devices are still constrained by their inability to respond to external mechanical pressure or sense human biomechanical movements over a broad working range. Additionally, we propose the development of new materials and device configurations with high piezoelectric coefficients and aligned electric dipole domains to improve the output of piezoelectric devices.[55,56,381] Since numerous amino acids and short peptides show significant piezoelectric characteristics in addition to outstanding bio-compatibility and bio-degradability, it would be intriguing to expand the piezoelectricity of such materials in the hydrogel state. Furthermore, extensive research is required to fully maximize the electrical output of piezoelectric hydrogels as this field is still in its early phases of development.

5.4 Wound healing/dressing

Hydrogel-based piezoelectric generators with biocompatible properties integrated into wearable self-powered treatments for wound healing or dressing have gained a lot of interest for medical applications. Due to their facile synthesis, low-cost fabrication, ease of portability, good wearability, and real-time effect, piezoelectric hydrogel-based PEGs have been demonstrated to have great potential in healthcare and biotechnology for the treatment of wounds. However, the developed piezoelectric hydrogels for wound dressing/healing have several limitations, such as flexibility, stretchability, permeability, and low antibacterial properties to support rapid wound healing. Another drawback of the piezoelectric hydrogels-based PEGs developed for wound healing is the poor endogenous bioelectricity due to the low piezoelectric properties of the piezopolymeric materials. Moreover, to the best of our knowledge, most of the P-PEGs are primarily based on piezopolymers and their composites, with no piezoelectric hydrogel-based PEGs (typically the hydrogels composed of amino acids and/or peptides) so far employed for wound healing/dressing. For future studies, high-performance and biocompatible piezoelectric hydrogels based on supramolecular organic and hybrid piezoelectric materials comprised of amino acids and/or peptides would be promising due to their high piezoelectricity and robust mechanical properties. Since amino acids and/or peptides are naturally chiral and biocompatible, they show piezoelectric properties that can promote self-supporting wound healing without the need for an external power supply. Moving forward, much work remains to be done in terms of appropriate material selection, piezoelectric response, and medical translation prospect, to develop piezoelectric hydrogels as a successful wound healing therapy.

5.5 Long-term stability and durability

In this review, piezoelectric hydrogel-based generators are highlighted as one of the most promising flexible energy harvesting and self-powered systems due to their multifunctionality. However, the poor stability and durability of the hydrogels pose a significant risk of shortening the detection accuracy and operational life of P-PEGs in case of a significant mechanical impact, crack development, friction, fatigue, humidity, radiation, high temperature, and chemical exposure, *etc.* Furthermore, the low mechanical strength and lack of strong polymer–polymer interactions in piezoelectric hydrogels compared to polymeric hydrogels have an impact on the long-term stability and output performance. Therefore, developing a robust strong network in hydrogels remains challenging for real-life applications of P-PEGs. To address these issues, many researchers employed polymeric materials such as polyimides (PI), polyvinyl chloride (PVC), polydimethylsiloxane (PDMS), and polytetrafluoroethylene (PTFE) to encapsulate the sensor device for enhancement of long-term durability.[18,382]

5.6 Powering electronics

Over the past few decades, the field of power harvesting and sensing has experienced substantial growth due to the increase in demand for portable and wireless electronics with long lifespans.[383,384] Currently, the powering of portable and wireless electronic devices still relies on rechargeable batteries. The usage of batteries can be challenging due to recycling and replacement issues as well as their short lifespan.[385,386] The concept of self-powered devices has significant advantages for the utilization of renewable energy sources, such as wind, waves, mechanical vibrations, breathing, blood flow, and other human-body movements.[387,388] Among various self-powered technologies, the most attractive portable devices and intelligent systems are based on piezoelectric hydrogels due to their combination of light-weight, high sensitivity, outstanding exceptional flexibility, skin-like mechanical characteristics and outstanding electrical properties. The piezoelectric hydrogels reported in this review showed considerable electrical characteristics such as voltage (typically ranging from 15 μV to 22 V), current (typically ranging from 0.21 nA to 2.8 μA), current density (typically ranging from 190 nA cm^{-2} to 220 nA cm^{-2}), and power density (typically ranging from 0.64 μW cm^{-2} to 1.7 mW m^{-2}), which are sufficient for powering many low-power portable electronics. For instance, the PUU-DH PiezoGel showed several prototype applications of LED lighting, object deformation detection and human motion detection demonstrating the potential uses in self-powered, wearable and artificial e-skin applications.[356] It is interesting to note that in another study, a piezoelectric hydrogel derived from ferroelectric PAN-PVDF revealed excellent piezoelectric coefficient (d_{33}, 30 pC N^{-1}), skin-like Young's modulus values (1.33–4.24 MPa), good stretchability (90–175%) and high toughness (1.23 MJ m^{-2}), indicating it as a promising material for artificial e-skin applications.[266] Moreover, the PiezoGel-based pressure sensor was shown to be capable of detecting physiological signals such as gestures, pulses, and spoken words.

Despite recent advances in piezoelectric hydrogel technology, the ability to power electronic devices based on these materials is still in its infancy. Overall, the output performances of PiezoGel-based devices reported so far are small compared to common piezoelectric materials. For implantable bio-electronic applications, the required average power typically ranges from 50 to 100 mW for stimulator devices (micro-actuators), 0.5 to 1.5 mW for communication system (ultrasonic transmitter) and <35 μW for biosensors (analog-to-digital converters).[385] At present, the majority of reported piezoelectric hydrogel-based devices lack sufficient powering capabilities to carry out several types of implantable bioelectronic applications. Moreover, by optimizing several factors, including selection of the appropriate piezo material, mechanical force, frequency, device area, poled and unpoled device structure, structural morphologies, and other structural defects (such as grain boundaries, growth domains, twins, dislocations, strain gradients, *etc.*), the output performance of the hydrogel-based piezoelectric devices can be enhanced. In particular, further research is required to develop PiezoGel materials and devices with high piezoelectric coefficient, high mechanical strength, good stretchability, high sensitivity and long-term stability, as well as superior fabrication methods and experimental standards. These important points should be taken into consideration when developing high piezoelectric devices to power electronic devices.

5.7 Bio-medical systems

By taking advantage of their soft, flexible, implantable and biocompatible nature, PiezoGels can be used in biomedical applications such as cardiac pacemakers, cardiac tachometers, drug pumps, cochlear implants, artificial retinas and stimulators (bone, muscle, nerve and brain). In addition, PiezoGels may be used as a diagnostic tool (temperature tracking, pulse frequency, respiration rate, and blood pressure monitoring) as well as a treatment for several types of health conditions (including stimulation of the brain and muscles). For powering implantable medical electronics, the voltage and power collected from the PiezoGel are very important for efficient operation. In general, the power and voltage requirements for implantable biomedical devices typically range from microwatt (μW)–milliwatt (mW) and 2–3 V, respectively.[389,390]

The first medical implanted device, the pacemaker, was developed using batteries that regulate the heartbeat using electrical impulses. So far, batteries are recognized as the most reliable power source for implantable medical electronics. However, due to size constraints and the battery's limited lifespan, it is challenging to reach long-term stability of implantable devices. For example, the battery system needs to be replaced after 7 to 10 years for a cardiac pacemaker and after 3–5 years for a deep brain stimulator. Another major health risk factor is the additional surgery required to replace the device (or battery).[391–395]

In this regard, self-powdered medical implants might be the best option by directly recharging the battery or harvesting biomechanical power from the movement of body organs such as cardiac motions.[396] An implantable cardiac pacemaker operates at an input of 100 μA and 3 V.[397] Many of the PiezoGel devices reported in this review show high piezoelectric charge coefficient, voltage, current, power density, and good bio-compatibility characteristics desirable for use in piezo-medicine (the use of piezoelectric materials in medicine) applications, particularly implantable sensors. Moreover, a systematic evaluation of the output performances including choice of piezo material, piezoelectric coefficient, applied mechanical force, area, thickness, voltage, current, current density and power density, would be beneficial in order to determine their viability for practical application and commercialization. Furthermore, to gain a complete understanding of this emerging area of research, valid benchmarking, comparison and consistency in data collection should be important considerations in future reports on PiezoGels-based devices.

Overall, progress on piezoelectric hydrogels for self-powered devices and bio-medical applications is still in its infancy stages. A significant emphasis should be directed to improving materials strength, flexibility, sensitivity, reliability, long-term stability and applicability. Despite these challenges, we believe that piezoelectric hydrogel-based self-powered systems will soon be widely used in biomedicine, portable electronics, electronic skin, and artificial intelligence. With a reliable multidisciplinary development effort in the search for cutting-edge bio-piezoelectric hydrogels and systems, it is envisioned that these newly developed platforms will enhance future intriguing green energy and healthcare applications.

Abbreviations

PEGs	Piezoelectric generators
PEHs	Piezoelectric energy harvesters
P-PEGs	PiezoGel-PEGs
$PbTiO_3$	Lead titanate
$BaTiO_3$	Barium titanate
$KNbO_3$	Potassium niobate

$PbZrTiO_3$	Lead zirconium titanate
PVDF	Poly-vinylidene fluoride
TrFE	Tri-fluoroethylene
HFP	Hexafluoropropylene
TeFE	Tetrafluoroethylene
CTFE	Chlorotrifluoroethylene
PA	Polyamides
PE	Polyesters
PUR	Polyurethane
PAN	Polyacrylonitrile
ZnO	Zinc oxide
ZnS	Zinc sulfide
CdS	Cadmium sulfide
AlN	Aluminum nitride
GaN	Gallium nitride
InN	Indium nitride
SnS	Tin monosulfide
MoS_2	Molybdenum disulfide
WSe_2	Tungsten diselenide
Pb	Lead
3D	Three-dimensional
ECM	Extracellular matrix
BAUS	Bioadhesive ultrasound
DNA	Deoxyribonucleic acid
PHEMA	Poly(2-hydroxyethyl methacrylate)
PVA	Polyvinyl alcohol
PVP	Polyvinylpyrrolidone
PEO	Polyethylene oxide
UPy	Acrylic acid-2-ureido-4-pyrimidone
PAM	Polyacrylamide
HA	Hyaluronic acid
SF	Silk fibroin
CS	Chitosan
TPU	Thermoplastic polyurethane
Dnase	Deoxyribonuclease
CF_2	Difluoromethylene
CN	Cyanide
PIP	Proximal interphalangeal joint
AN	Acrylonitrile
NaSS	Sodium p-styrenesulfonate
MBA	Methylene-bis-acrylamide
APS	Ammonium persulfate
DMSO	Dimethyl sulfoxide
H_2O	Water
GO	Graphene oxide
SWCNTs	Single-walled carbon nanotubes
MWCNTs	Multi-walled carbon nanotubes
DA	Diacrylate
CEA	Carboxyethyl acrylate
SA	Sodium-alginate
DBP	Dibutyl phthalate
LiCl	Lithium chloride
p(NVCL-*co*-DEGDVE)	Poly-*N*-vinylcaprolactamco-di(ethylene glycol) divinyl ether
CHACC	Chitosan quaternary ammonium salt
AM	Acrylamide
MA	Maleic acid
Fe^{3+}	Ferric ion
NPs	Nanoparticles
FT-IR	Fourier transform infrared spectroscopy
SEM	Scanning electron microscopy
GT	Granulation tissue
EG	Epithelium gap
RBC	Regenerated bacterial cellulose
NdFeB	Neodymium magnet
CBM	Carbomer
CMCS	Carboxymethyl chitosan
TA	Tannic acid
FWO	$FeWO_4$
Ag	Silver
PIs	Pressure injuries
PUs	Pressure ulcers
HUVEC	Human umbilical vein endothelial cells
Gel	Gelatin
OCS	Oxychondroitin sulfate
A-BTO	Aminated-BTO
PEGDA	poly(ethylene glycol) diacrylate
Au-BTO	Gold-nanoparticle-decorated-BTO
GelMA	Methacrylate gelatin
US	Ultrasound
ROS	Reactive oxygen species
VEGF	Vascular endothelial growth factor
UV	Ultraviolet
$CaCl_2$	Calcium chloride
LEDs	Light-emitting diodes
t	Thickness
D	Diameter
FF	Diphenylalanine
Fmoc-FF	Fluorenylmethoxycarbonyldiphenylalanine
dabco$HReO_4$ or DH	1,4-diazabicyclo[2.2.2]octane perrhenate
PUU	Poly(urethane-urea)
Im-ClO_4	Imidazolium perchlorate
L-PFM	Lateral piezoresponse force microscopy
PI	Polyimides
PVC	Polyvinyl chloride
PDMS	Polydimethylsiloxane
PTFE	Polytetrafluoroethylene

Conflicts of interest

There are no conflicts to declare.

Acknowledgements

T. V. thanks Tel Aviv University for the post-doctoral fellowship. E. G. acknowledges the support of the European Research Council PoC project PiezoGel (966813) and PepZoPower (101101071). Views and opinions expressed are however those of the author only and do not necessarily reflect those of the European Union or the European Research Council. Neither the

European Union nor the granting authority can be held responsible for them.

References

1 M. J. Cima, *Nat. Biotechnol.*, 2014, **32**, 642–643.
2 G. Chen, Y. Li, M. Bick and J. Chen, *Chem. Rev.*, 2020, **120**, 3668–3720.
3 H. Kim, K. R. Pyun, M. T. Lee, H. B. Lee and S. H. Ko, *Adv. Funct. Mater.*, 2022, **32**, 2110535.
4 A. S. Torralba, R. Álvarez-Diduk, C. Parolo, A. Piper and A. Merkoçi, *Chem. Rev.*, 2022, **122**, 14881–14910.
5 M. Veletic, E. H. Apu, M. Simic, J. Bergsland, I. Balasingham, C. H. Contag and N. Ashammakhi, *Chem. Rev.*, 2022, **122**, 16329–16363.
6 S. Shrivastava, T. T. Quang and N. E. Lee, *Chem. Soc. Rev.*, 2020, **49**, 1812–1866.
7 G. Chen, X. Xiao, X. Zhao, T. Tat, M. Bick and J. Chen, *Chem. Rev.*, 2022, **122**, 3259–3291.
8 N. A. Kyeremateng, T. Brousse and D. Pech, *Nat. Nanotechnol*, 2017, **12**, 7–15.
9 P. Simon and Y. Gogotsi, *Nat. Mater.*, 2020, **19**, 1151–1163.
10 R. Zhu, S. Murali, M. D. Stoller, K. J. Ganesh, W. Cai, P. J. Ferreira, A. Pirkle, R. M. Wallace, K. A. Cychosz, M. Thommes, D. Su, E. A. Stach and R. S. Ruoff, *Science*, 2011, **332**, 1537–1541.
11 M. F. El-Kady, V. Strong, S. Dubin and R. B. Kaner, *Science*, 2012, **335**, 1326–1330.
12 S. J. Varma, K. S. Kumar, S. Seal, S. Rajaraman and J. Thomas, *Adv. Sci*, 2018, **5**, 1800340.
13 C. R. Bowen, H. A. Kim, P. M. Weaver and S. Dunn, *Energy Environ. Sci.*, 2014, **7**, 25–44.
14 O. Ellabban, H. Abu-Rub and F. Blaabjerg, *Renewable Sustainable Energy Rev*, 2014, **39**, 748–764.
15 S. D. Mahapatra, P. C. Mohapatra, A. I. Aria, G. Christie, Y. K. Mishra, S. Hofmann and V. K. Thakur, *Adv. Sci*, 2021, **8**, 2100864.
16 A. Toprak and O. Tigli, *Appl. Phys. Rev*, 2014, **1**, 031104.
17 Y. Y. Tang, P. F. Li, W. Q. Liao, P. P. Shi, Y. M. You and R. G. Xiong, *J. Am. Chem. Soc.*, 2018, **140**, 8051–8059.
18 H. A. Sodano, D. J. Inman and G. Park, *Shock and Vibration Digest*, 2004, **36**, 197–206.
19 H. Li, C. Tian and Z. D. Deng, *Appl. Phys. Rev*, 2014, **1**, 041301.
20 X. Zhou, G. Xue, H. Luo, C. R. Bowen and D. Zhang, *Prog. Mater. Sci.*, 2021, **122**, 100836.
21 N. Sezer and M. Koc, *Nano Energy*, 2021, **80**, 105567.
22 Z. L. Wang and J. Song, *Science*, 2006, **312**, 242–246.
23 J. Li and X. Wang, *APL Mater*, 2017, **5**, 073801.
24 K. I. Park, C. K. Jeong, N. K. Kim and K. J. Lee, *Nano Convergence*, 2016, **3**, 12.
25 C. A. P. de Araujo, J. D. Cuchiaro, L. D. McMillan, M. C. Scott and J. F. Scott, *Nature*, 1995, **374**, 627–629.
26 S. Das and J. Appenzeller, *Nano Lett*, 2011, **11**, 4003–4007.
27 J. F. Scott, *Science*, 2007, **315**, 954–959.
28 L. W. Martin and A. M. Rappe, *Nat. Rev. Mater*, 2017, **2**, 16087.
29 Y. Bai, H. Jantunen and J. Juuti, *Adv. Mater.*, 2018, **30**, 1707271.
30 M. Abbasipour, R. Khajavi and A. Akbarzadeh, *Adv. Eng. Mater.*, 2022, **24**, 2101312.
31 K. S. Ramadan, D. Sameoto and S. Evoy, *Smart Mater. Struct.*, 2014, **23**, 033001.
32 X. Cao, Y. Xiong, J. Sun, X. Zhu, Q. Sun and Z. L. Wang, *Adv. Funct. Mater.*, 2021, **31**, 2102983.
33 B. C. K. Tee, C. Wang, R. Allen and Z. Bao, *Nat. Nanotechnol*, 2012, **7**, 825–832.
34 A. Chortos, J. Liu and Z. Bao, *Nat. Mater.*, 2016, **15**, 937–950.
35 C. Wu, A. C. Wang, W. Ding, H. Guo and Z. L. Wang, *Adv. Energy Mater*, 2019, **9**, 1802906.
36 W. Gao, H. Ota, D. Kiriya, K. Takei and A. Javey, *Acc. Chem. Res.*, 2019, **52**, 523–533.
37 Z. L. Wang, J. Chen and L. Lin, *Energy Environ. Sci.*, 2015, **8**, 2250–2282.
38 J. H. Park, H. E. Lee, C. K. Jeong, D. H. Kim, S. K. Hong, K. I. Park and K. J. Lee, *Nano Energy*, 2019, **56**, 531–546.
39 T. Vijayakanth, D. J. Liptrot, E. Gazit, R. Boomishankar and C. R. Bowen, *Adv. Funct. Mater.*, 2022, **32**, 2109492.
40 W. Deng, Y. Zhou, A. Libanori, G. Chen, W. Yang and J. Chen, *Chem. Soc. Rev.*, 2022, **51**, 3380–3435.
41 J. Briscoe and S. Dunn, *Nano Energy*, 2015, **14**, 15–29.
42 Y. Hu and Z. L. Wang, *Nano Energy*, 2015, **14**, 3–14.
43 Y. Zhang, M. Xie, V. Adamaki, H. Khanbareh and C. R. Bowen, *Chem. Soc. Rev.*, 2017, **46**, 7757–7786.
44 T. Vijayakanth, A. K. Srivastava, F. Ram, P. Kulkarni, K. Shanmuganathan, B. Praveenkumar and R. Boomishankar, *Angew. Chem., Int. Ed.*, 2018, **57**, 9054–9058.
45 T. Vijayakanth, F. Ram, B. Praveenkumar, K. Shanmuganathan and R. Boomishankar, *Chem. Mater.*, 2019, **31**, 5964–5972.
46 V. Jella, S. Ippili, J. H. Eom, S. V. N. Pammi, J. S. Jung, V. D. Tran, V. H. Nguyen, A. Kirakosyan, S. Yun, D. Kim, M. R. Sihn, J. Choi, Y. J. Kim, H. J. Kim and S. G. Yoon, *Nano Energy*, 2019, **57**, 74–93.
47 T. Vijayakanth, F. Ram, B. Praveenkumar, K. Shanmuganathan and R. Boomishankar, *Angew. Chem., Int. Ed.*, 2020, **59**, 10368–10373.
48 H. Park, C. Ha and J. H. Lee, *J. Mater. Chem. A*, 2020, **8**, 24353–24367.
49 T. Vijayakanth, S. Sahoo, P. Kothavade, V. Bhan Sharma, D. Kabra, J. K. Zaręba, K. Shanmuganathan and R. Boomishankar, *Angew. Chem. Int. Ed.*, 2023, **62**, e202214984.
50 D. Kim, S. A. Han, J. H. Kim, J. H. Lee, S. W. Kim and S. W. Lee, *Adv. Mater.*, 2020, **32**, e1906989.
51 Q. Xu, X. Gao, S. Zhao, Y. N. Liu, D. Zhang, K. Zhou, H. Khanbareh, W. Chen, Y. Zhang and C. Bowen, *Adv. Mater.*, 2021, **33**, 2008452.
52 F. Ram, J. Garemark, Y. Li, T. Pettersson and L. A. Berglund, *ACS Nano*, 2022, **16**, 15805–15813.
53 S. Panda, S. Hajra, K. Mistewicz, P. In-na, M. Sahu, P. M. Rajaitha and H. J. Kim, *Nano Energy*, 2022, **100**, 107514.
54 Y. C. Jeong, H. E. Lee, A. Shin, D. G. Kim, K. J. Lee and D. Kim, *Adv. Mater.*, 2020, **32**, 1907522.

55 S. Bera, S. Guerin, H. Yuan, J. O'Donnell, N. P. Reynolds, O. Maraba, W. Ji, L. J. W. Shimon, P. A. Cazade, S. A. M. Tofail, D. Thompson, R. Yang and E. Gazit, *Nat. Commun.*, 2021, **12**, 2634.

56 V. Basavalingappa, S. Bera, B. Xue, J. O'Donnell, S. Guerin, P. A. Cazade, H. Yuan, E. U. Haq, C. Silien, K. Tao, L. J. W. Shimon, S. A. M. Tofail, D. Thompson, S. Kolusheva, R. Yang, Y. Cao and E. Gazit, *ACS Nano*, 2020, **14**, 7025–7037.

57 Y. Chen, S. Guerin, H. Yuan, J. O'Donnell, B. Xue, P. A. Cazade, E. U. Haq, L. J. W. Shimon, S. Rencus-Lazar, S. A. M. Tofail, Y. Cao, D. Thompson, R. Yang and E. Gazit, *J. Am. Chem. Soc.*, 2022, **144**, 3468–3476.

58 S. Guerin, A. Stapleton, D. Chovan, R. Mouras, M. Gleeson, C. McKeown, M. R. Noor, C. Silien, F. M. F. Rhen, A. L. Kholkin, N. Liu, T. Soulimane, S. A. M. Tofail and D. Thompson, *Nat. Mater.*, 2018, **17**, 180–186.

59 P. S. Zelenovskii, K. Romanyuk, M. S. Liberato, P. Brandão, F. F. Ferreira, S. Kopyl, L. M. Mafra, W. A. Alves and A. L. Kholkin, *Adv. Funct. Mater.*, 2021, **31**, 2102524.

60 T. Shimizu, W. Ding and N. Kameta, *Chem. Rev.*, 2020, **120**, 2347–2407.

61 M. T. Chorsi, E. J. Curry, H. T. Chorsi, R. Das, J. Baroody, P. K. Purohit, H. Ilies and T. D. Nguyen, *Adv. Mater.*, 2019, **31**, 1802084.

62 F. Yang, J. Li, Y. Long, Z. Zhang, L. Wang, J. Sui, Y. Dong, Y. Wang, R. Taylor, D. Ni, W. Cai, P. Wang, T. Hacker and X. Wang, *Science*, 2021, **373**, 337–342.

63 J. C. Anderson and C. Eriksson, *Nature*, 1970, **227**, 491–492.

64 R. Wang, J. Sui and X. Wang, *ACS Nano*, 2022, **16**, 17708–17728.

65 S. T. Yucel, P. Cebe and D. L. Kaplan, *Adv. Funct. Mater.*, 2011, **21**, 779–785.

66 Y. M. Mei, Q. F. Zeng, L. He, P. Yin, Y. Sun, W. Hu and R. Yang, *iScience*, 2021, **24**, 102274.

67 E. Fukada, Piezoelectricity as a fundamental property of wood, *Wood Sci. Technol.*, 1968, **2**, 299–307.

68 C. A. L. Bassett and R. O. Becker, *Science*, 1962, **137**, 1063–1064.

69 S. Rajala, T. Siponkoski, E. Sarlin, M. Mettänen, M. Vuoriluoto, A. Pammo, J. Juuti, O. J. Rojas, S. Franssila and S. Tuukkanen, *ACS Appl. Mater. Interfaces*, 2016, **8**, 15607–15614.

70 H. Wu, Y. Huang, F. Xu, Y. Duan and Z. Yin, *Adv. Mater.*, 2016, **28**, 9881–9919.

71 E. M. Ahmed, *J. Adv. Res*, 2015, **6**, 105–121.

72 Y. S. Zhang and A. Khademhosseini, *Science*, 2017, **356**, eaaf3627.

73 C. Wang, T. Yokota and T. Someya, *Chem. Rev.*, 2021, **121**, 2109–2146.

74 T. Jungst, W. Smolan, K. Schacht, T. Scheibel and J. Groll, *Chem. Rev.*, 2016, **116**, 1496–1539.

75 S. Correa, A. K. Grosskopf, H. Lopez Hernandez, D. Chan, A. C. Yu, L. M. Stapleton and E. A. Appel, *Chem. Rev.*, 2021, **121**, 11385–11457.

76 Y. Du, W. Du, D. Lin, M. Ai, S. Li and L. Zhang, *Micromachines*, 2023, **14**, 167.

77 B. X. Wang, W. Xu, Z. Yang, Y. Wu and F. Pi, *Macromol. Rapid Commun.*, 2022, **43**, 2100785.

78 J. T. Nguyen and W. Cheng, *Small Struct*, 2022, **3**, 2200034.

79 M. E. Lines and A. M. Glass, *Principles and Applications of Ferroelectrics and Related Materials*, Oxford University Press, New York, 1977.

80 F. Sheehan, D. Sementa, A. Jain, M. Kumar, M. TayaraniNajjaran, D. Kroiss and R. V. Ulijn, *Chem. Rev.*, 2021, **121**, 13869–13914.

81 J. Zhang, Y. Wang, B. J. Rodriguez, R. Yang, Y. Bin, D. Mei, J. Li, K. Tao and E. Gazit, *Chem. Soc. Rev.*, 2022, **51**, 6936–6947.

82 J. Jacob, N. More, K. Kalia and G. Kapusetti, *Inflamm. Regen*, 2018, **38**, 1–11.

83 K. Kapat, Q. T. H. Shubhra, M. Zhou and S. Leeuwenburgh, *Adv. Funct. Mater.*, 2020, **30**, 1909045.

84 Z. Liu, X. Wan, Z. L. Wang and L. Li, *Adv. Mater.*, 2021, **33**, 2007429.

85 F. C. Kao, H. H. Ho, P. Y. Chiu, M. K. Hsieh, J. Liao, P. L. Lai, Y. F. Huang, M. Y. Dong, T. T. Tsai and Z. H. Lin, *Sci. Technol. Adv. Mater.*, 2022, **23**, 1–16.

86 J. Valasek, *Phys. Rev*, 1921, **17**, 475–481.

87 G. Busch and P. Scherrer, *Naturwissenschaften*, 1935, **23**, 737–738.

88 T. Hang, W. Zhang, H. Y. Ye and R. G. Xiong, *Chem. Soc. Rev.*, 2011, **40**, 3577–3598.

89 J. Chen, Q. Qiu, Y. Han and D. Lau, *Renewable and Sustainable Energy Reviews*, 2019, **101**, 14–25.

90 H. Y. Liu, H. Y. Zhang, X. G. Chen and R. G. Xiong, *J. Am. Chem. Soc.*, 2020, **142**, 15205–15218.

91 J. Curie and P. Curie, *Bulletin de Mineralogie*, 1880, **3**, 90–93.

92 P. P. Shi, Y. Y. Tang, P. F. Li, W. Q. Liao, Z. X. Wang, Q. Ye and R. G. Xiong, *Chem. Soc. Rev.*, 2016, **45**, 3811–3827.

93 H. Y. Zhang, Y. Y. Tang, P. P. Shi and R. G. Xiong, *Acc. Chem. Res.*, 2019, **52**, 1928–1938.

94 Z. L. Wang, *Mater. Today*, 2017, **20**, 74–82.

95 K. M. Ok, E. O. Chi and P. S. Halasyamani, *Chem. Soc. Rev.*, 2006, **35**, 710–717.

96 P. Dineva, D. Gross, R. Müller and T. Rangelov, Piezoelectric Materials. *Dynamic Fracture of Piezoelectric Materials*, Springer, 2014, pp. 7–32.

97 K. Uchino, *Advanced Piezoelectric Materials*, Woodhead Publishing, 2017, pp. 385–451.

98 T. R. Ray, J. Choi, A. J. Bandodkar, S. Krishnan, P. Gutruf, L. Tian, R. Ghaffari and J. A. Rogers, *Chem. Rev.*, 2019, **119**, 5461–5533.

99 Z. Yang, S. Zhou, J. Zu and D. Inman, *Joule*, 2018, **2**, 642–697.

100 D. Hu, M. Yao, Y. Fan, C. Ma, M. Fan and M. Liu, *Nano energy*, 2019, **55**, 288–304.

101 C. C. Kim, H. H. Lee, K. H. Oh and J. Y. Sun, *Science*, 2016, **353**, 682–687.

102 C. Yang and Z. Suo, *Nat. Rev. Mater*, 2018, **3**, 125–142.

103 C. Larson, B. Peele, S. Li, S. Robinson, M. Totaro, L. Beccai, B. Mazzolai and R. Shepherd, *Science*, 2016, **351**, 1071–1074.

104 J. Odent, T. J. Wallin, W. Pan, K. Kruemplestaedter, R. F. Shepherd and E. P. Giannelis, *Adv. Funct. Mater.*, 2017, **27**, 1701807.

105 C. Laschi, B. Mazzolai and M. Cianchetti, *Sci. Robot.*, 2016, **1**, eaah3690.
106 S. Huang, Y. Liu, Y. Zhao, Z. Ren and C. F. Guo, *Adv. Funct. Mater.*, 2019, **29**, 1805924.
107 A. Burd, *Ostomy Wound Manag*, 2007, **53**, 52–62.
108 C. Wang, X. Chen, L. Wang, M. Makihata, H. C. Liu, T. Zhou and X. Zhao, *Science*, 2022, **377**, 517–523.
109 S. F. Bernatchez, *J. Vasc. Access*, 2014, **19**, 256–261.
110 L. Wang, Z. Lou, K. Jiang and G. Shen, *Adv. Intell. Syst*, 2019, **1**, 1900040.
111 H. Yuk, B. Lu and X. Zhao, *Chem. Soc. Rev.*, 2019, **48**, 1642–1667.
112 X. Zhao, X. Chen, H. Yuk, S. Lin, X. Liu and G. Parada, *Chem. Rev.*, 2021, **121**, 4309–4372.
113 H. Yuk, J. Wu and X. H. Zhao, *Nat. Rev. Mater*, 2022, **7**, 935–952.
114 X. Kuang, M. O. Arıcan, T. Zhou, X. Zhao and Y. S. Zhang, *Acc. Mater. Res*, 2023, **4**, 101–114.
115 Y. Guo, J. Bae, Z. Fang, P. Li, F. Zhao and G. Yu, *Chem. Rev.*, 2020, **120**, 7642–7707.
116 G. Su, J. Cao, X. Zhang, Y. Zhang, S. Yin, L. Jia, Q. Guo, X. Zhang, J. Zhang and T. Zhou, *J. Mater. Chem. A*, 2020, **8**, 2074–2082.
117 A. Herrmann, R. Haag and U. H. Schedler, *Adv. Healthcare Mater*, 2021, **10**, 2100062.
118 Z. Meng, Q. Liu, Y. Zhang, J. Sun, C. Yang, H. Li, M. Loznik, R. Gostl, D. Chen, F. Wang, N. A. Clark, H. Zhang, A. Herrmann and K. Liu, *Adv. Mater.*, 2022, **34**, 2106208.
119 D. Wirthl, R. Pichler, M. Drack, G. Kettlguber, R. Moser, R. Gerstmayr, F. Hartmann, E. Bradt, R. Kaltseis, C. M. Siket, S. E. Schausberger, S. Hild, S. Bauer and M. Kaltenbrunner, *Sci. Adv*, 2017, **3**, e1700053.
120 I. Jeon, J. Cui, W. R. K. Illeperuma, J. Aizenberg and J. J. Vlassak, *Adv. Mater.*, 2016, **28**, 4678–4683.
121 J. Y. Sun, X. Zhao, W. R. K. Illeperuma, O. Chaudhuri, K. H. Oh, D. J. Mooney, J. J. Vlassak and Z. Suo, *Nature*, 2012, **489**, 133–136.
122 H. Montazerian, E. Davoodi, A. Baidya, M. Badv, R. Haghniaz, A. Dalili, A. S. Milani, M. Hoorfar, N. Annabi, A. Khademhosseini and P. S. Weiss, *Chem. Soc. Rev.*, 2022, **51**, 9127–9173.
123 J. Luo, J. J. Yang, X. R. Zheng, X. Ke, Y. T. Chen, H. Tan and J. S. Li, *Adv. Healthcare Mater*, 2020, **9**, 1901423.
124 X. D. Wang, J. H. Song, J. Liu and Z. L. Wang, *Science*, 2007, **316**, 102–105.
125 Y. Wang, M. Hong, J. Venezuela, T. Liu and M. Dargusch, *Bioact. Mater.*, 2023, **22**, 291–311.
126 S. Gong and W. L. Cheng, *Adv. Energy Mater*, 2017, **7**, 1700648.
127 J. S. Kahn, Y. Hu and I. Willner, *Acc. Chem. Res.*, 2017, **50**, 680–690.
128 M. E. Allen, J. W. Hindley, D. K. Baxani, O. Ces and Y. Elani, *Nat. Rev. Chem*, 2022, **6**, 562.
129 P. Makam, S. P. Senanayak, K. S. Narayan and T. Govindaraju, *J. Am. Chem. Soc.*, 2016, **138**, 8259–8268.
130 P. Makam and E. Gazit, *Chem. Soc. Rev.*, 2018, **47**, 3406–3420.
131 S. M. M. Reddy, G. Augustine, N. Ayyadurai and G. Shanmugam, *ACS Appl. Bio Mater*, 2018, **1**, 1382–1388.
132 N. Sood, A. Bhardwaj, S. Mehta and A. Mehta, *Drug Delivery*, 2016, **23**, 758–780.
133 H. M. El-Husseiny, E. A. Mady, W. A. El-Dakroury, M. B. Zewail, M. Noshy, A. M. Abdelfatah and A. S. Doghish, *Appl. Mater. Today*, 2022, **13**, 101560.
134 I. Willner, *Acc. Chem. Res.*, 2017, **50**(4), 657–658.
135 M. C. Koetting, J. T. Peters, S. D. Steichen and N. A. Peppas, *Mater. Sci. Eng., R*, 2015, **93**, 1–49.
136 D. K. Duraisamy, P. D. Sureshbhai, P. Saveri, A. P. Deshpande and G. Shanmugam, *Chem. Commun.*, 2022, **58**, 13377.
137 B. Roy and T. Govindaraju, *Bull. Chem. Soc. Jpn.*, 2019, **92**, 1883–1901.
138 S. M. M. Reddy, P. Dorishetty, G. Augustine, A. P. Deshpande, N. Ayyadurai and G. Shanmugam, *Langmuir*, 2017, **33**, 13504–13514.
139 S. Mukherjee and G. Shanmugam, *Small*, 2023, 2206906, DOI: 10.1002/smll.202206906.
140 F. G. Downs, D. J. Lunn, M. J. Booth, J. B. Sauer, W. J. Ramsay, R. G. Klemperer, C. J. Hawker and H. Bayley, *Nat. Chem*, 2020, **12**, 363–371.
141 M. Niazi, E. Alizadeh, A. Zarebkohan, K. Seidi, M. H. AyoubiJoshaghani, M. Azizi, H. Dadashi, H. Mahmudi, T. Javaheri, M. Jaymand, M. R. Hamblin, R. J. Esfahlan and Z. Amoozgar, *Adv. Funct. Mater.*, 2021, **31**, 2104123.
142 X. Liu, M. Gao, J. Chen, S. Guo, W. Zhu, L. Bai, W. Zhai, H. Du, H. Wu, C. Yan, Y. Shi, J. Gu, H. J. Qi and K. Zhou, *Adv. Funct. Mater.*, 2022, **32**, 2203323.
143 Y. Long, H. Wei, J. Li, G. Yao, B. Yu, D. Ni, A. L. Gibson, X. Lan, Y. Jiang, W. Cai and X. Wang, *ACS Nano*, 2018, **12**, 12533–12540.
144 B. Song, Y. Gu, J. Pu, B. Reid, Z. Zhao and M. Zhao, *Nat. Protoc.*, 2007, **2**, 1479.
145 K. Dong, X. Peng and Z. L. Wang, *Adv. Mater.*, 2020, **32**, 1902549.
146 C. Qin, Z. Yue, G. G. Wallace and J. Chen, *ACS Appl. Bio Mater*, 2022, **5**, 5041–5056.
147 S. Kopyl, R. Surmenev, M. Surmeneva, Y. Fetisov and A. Kholkin, *Mater. Today Bio*, 2021, **12**, 100149.
148 Z. Liu, J. Fan, M. Zou, X. Ma, Y. Niu and G. Gong, *ChemistrySelect*, 2021, **6**, 11931–11938.
149 T. Zhu, Y. Ni, G. M. Biesold, Y. Cheng, M. Ge, H. Li, J. Huang, Z. Lin and Y. Lai, *Chem. Soc. Rev.*, 2023, **52**, 473–509.
150 J. Li and D. J. Mooney, *Nat. Rev. Mater*, 2016, **1**, 16071.
151 H. M. Khan, X. Liao, B. A. Sheikh, Y. Wang, Z. Su, C. Guo, Z. Li, C. Zhou, Y. Cen and Q. Kong, *J. Mater. Chem. B*, 2022, **10**, 6859–6895.
152 K. O. Rojek, M. Ćwiklińska, J. Kuczak and J. Guzowski, *Chem. Rev.*, 2022, **122**, 16839–16909.
153 C. Wang, E. S. Sani and W. Gao, *Adv. Funct. Mater.*, 2022, **32**, 2111022.
154 Y. Liang, J. He and B. Guo, *ACS Nano*, 2021, **15**, 12687–12722.

155 S. Khosravimelal, M. Mobaraki, S. Eftekhari, M. Ahearne, A. M. Seifalian and M. Gholipourmalekabadi, *Small*, 2021, **17**, 2006335.
156 A. M. Vargason, A. C. Anselmo and S. Mitragotri, *Nat. Biomed. Eng*, 2021, **5**, 951–967.
157 Y. Zhu, S. Li, J. Li, N. Falcone, Q. Cui, S. Shah, M. C. Hartel, N. Yu, P. Young, N. R. Barros, Z. Wu, R. Haghniaz, M. Ermis, C. Wang, H. Kang, J. Lee, S. Karamikamkar, S. Ahadian, V. Jucaud, M. R. Dokmeci, H. J. Kim and A. Khademhosseini, *Adv. Mater.*, 2022, **34**, 2108389.
158 L. Jones, A. Hui, C. M. Phan, M. L. Read, D. Azar, J. Buch, J. B. Ciolino, S. A. Naroo, B. Pall, K. Romond, P. Sankaridurg, C. M. Schnider, L. Terry and M. Willcox, *Contact Lens and Anterior Eye*, 2021, **44**, 398–430.
159 X. Liu, H. Yu, L. Wang, Z. Huang, F. Haq, L. Teng, M. Jin and B. Ding, *Adv. Mater. Interfaces*, 2022, **9**, 2101038.
160 X. Li, Y. Lu and Y. Hu, *Matter*, 2022, **5**, 2473–2475.
161 S. Fathizadeh and S. Behnia, *J. Phys. Soc. Jpn.*, 2020, **89**, 024004.
162 F. Lucarelli, S. Tombelli, M. Minunni, G. Marrazza and M. Mascini, *Anal. Chim. Acta*, 2008, **609**, 139–159.
163 Y. Wei, K. Wang, S. Luo, F. Li, X. Zuo, C. Fan and Q. Li, *Small*, 2022, **18**, 2107640–2107653.
164 M. Pohanka, *Materials*, 2018, **11**, 448.
165 Z. Xiong, S. Achavananthadith, S. Lian, L. E. Madden, Z. X. Ong, W. Chua, V. Kalidasan, Z. Li, Z. Liu, P. Singh, H. Yang, S. P. Heussler, S. M. P. Kalaiselvi, M. B. H. Breese, H. Yao, Y. Gao, K. Sanmugam, B. C. K. Tee, P. Y. Chen, W. Loke, C. T. Lim, G. S. H. Chiang, B. Y. Tan, H. Li, D. L. Becker and J. S. Ho, *Sci. Adv.*, 2021, **7**, eabj1617.
166 M. Zarei, G. Lee, S. G. Lee and K. Cho, *Adv. Mater.*, 2023, **35**, 2203193.
167 E. Caló and V. V. Khutoryanskiy, *Eur. Polym. J.*, 2015, **65**, 252–267.
168 F. Ullah, M. B. H. Othman, F. Javed, Z. Ahmad and H. M. Akil, *Mater. Sci. Eng., C*, 2015, **57**, 414–433.
169 Y. Li, J. Rodrigues and H. Tomas, *Chem. Soc. Rev.*, 2012, **41**, 2193–2221.
170 Y. Cao and R. Mezzenga, *Nat. Food*, 2020, **1**, 106–118.
171 E. S. Hosseini, S. Dervin, P. Ganguly and R. Dahiya, *ACS Appl. Bio Mater*, 2021, **4**, 163–194.
172 J. Li, Y. Long, F. Yang and X. Wang, *Curr. Opin. Solid State Mater. Sci*, 2020, **24**, 100806.
173 Y. Zhu, R. Haghniaz, M. C. Hartel, L. Mou, X. Tian, P. R. Garrido, Z. Wu, T. Hao, S. Guan, S. Ahadian, H. J. Kim, V. Jucaud, M. R. Dokmeci and A. Khademhosseini, *ACS Biomater. Sci. Eng*, 2023, **9**, 2048–2069.
174 S. Hu, M. Zheng, Q. Wang, L. Li, J. Xing, K. Chen, F. Qi, P. He, L. Mao, Z. Shi, B. Su and G. Yang, *Carbohydr. Polym*, 2022, **298**, 120115.
175 H. Liu, J. Zhong, C. Lee, S. W. Lee and L. Lin, *Appl. Phys. Rev*, 2018, **5**, 041306.
176 V. Vallem, Y. Sargolzaeiaval, M. Ozturk, Y. C. Lai and M. D. Dickey, *Adv. Mater.*, 2021, **33**, 2004832.
177 H. C. Song, S. W. Kim, H. S. Kim, D. G. Lee, C. Y. Kang and S. Nahm, *Adv. Mater.*, 2020, **32**, 2002208.
178 H. R. Lim, H. S. Kim, R. Qazi, Y. T. Kwon, J. W. Jeong and W. H. Yeo, *Adv. Mater.*, 2020, **32**, 1901924.
179 A. G. Athanassiadis, Z. Ma, N. M. Gomez, K. Melde, E. Choi, R. Goyal and P. Fischer, *Chem. Rev.*, 2022, **122**, 5165–5208.
180 M. Su and Y. Song, *Chem. Rev.*, 2022, **122**, 5144–5164.
181 R. Anton and H. A. Sodano, *Smart Mater. Struct.*, 2007, **16**, R1–R21.
182 L. Yin, K. N. Kim, A. Trifonov, T. Podhajny and J. Wang, *Energy Environ. Sci.*, 2022, **15**, 82–101.
183 S. Gupta, W. T. Navaraj, L. Lorenzelli and R. Dahiya, *NPJ Flexible Electron*, 2018, **2**, 1–17.
184 N. A. Shepelin, A. M. Glushenkov, V. C. Lussini, P. J. Fox, G. W. Dicinoski, J. G. Shapter and A. V. Ellis, *Energy Environ. Sci.*, 2019, **12**, 1143–1176.
185 S. V. Fernandez, F. Cai, S. Chen, E. Suh, J. Tiepelt, R. McIntosh, C. Marcus, D. Acosta, D. Mejorado and C. Dagdeviren, *ACS Biomater. Sci. Eng*, 2023, **9**, 2070–2086.
186 Y. J. Gong, Z. G. Li, H. Chen, T. M. Guo, F. F. Gao, G. J. Chen, Y. Zhang, Y. M. You, W. Li, M. He, X. H. Bu and J. Yu, *Matter*, 2023, **6**, 2066–2080.
187 T. M. Guo, Y. J. Gong, Z. G. Li, Y. M. Liu, W. Li, Z. Y. Li and X. H. Bu, *Small*, 2022, **18**, 2103829.
188 Y. Zhao, L. C. An, K. Li, Y. J. Gong, T. M. Guo, F. F. Gao, Y. Lei, Q. Li, W. Li and X. H. Bu, *Sci. China Mater*, 2023, **66**, 1854–1860.
189 T. Vijayakanth, R. Pandey, P. Kulkarni, B. Praveenkumar, D. Kabra and R. Boomishankar, *Dalton Trans.*, 2019, **48**, 7331–7336.
190 S. Amirthalingam, A. K. Rajendran, Y. G. Moon and N. Hwang, *Mater. Horiz*, 2023, DOI: 10.1039/D3MH00399J.
191 F. J. Tovar-Lopez, *Sensors*, 2023, **23**, 5406.
192 M. Xu, S. Wu, L. Ding, C. Lu, H. Qian, J. Qu and Y. Chen, *J. Mater. Chem. B*, 2023, **11**, 4318–4329.
193 C. Zhang, M. O. G. Nayeem, Z. Wang, X. Pu, C. Dagdeviren, Z. L. Wang, X. Zhang and R. Liu, *Progress in Materials Science*, 2023, **138**, 101156.
194 B. K. Sun, Z. Siprashvili and P. A. Khavari, *Science*, 2014, **346**, 941–945.
195 S. Saghazadeh, C. Rinoldi, M. Schot, S. S. Kashaf, F. Sharifi, E. Jalilian, K. Nuutila, G. Giatsidis, P. Mostafalu, H. Derakhshandeh, K. Yue, W. Swieszkowski, A. Memic, A. Tamayol and A. Khademhosseini, *Adv. Drug Delivery Rev*, 2018, **127**, 138–166.
196 A. Maleki, J. H. He, S. Bochani, V. Nosrati, M. A. Shahbazi and B. L. Guo, *ACS Nano*, 2021, **15**, 18895–18930.
197 J. Koehler, F. P. Brandl and A. M. Goepferich, *Eur. Polym. J.*, 2018, **100**, 1–11.
198 S. Hamdan, I. Pastar, S. Drakulich, E. Dikici, M. Tomic-Canic, S. Deo and S. Daunert, *ACS Cent. Sci*, 2017, **3**, 163–175.
199 X. Deng, M. Gould and M. A. Ali, *J. Biomed. Mater. Res.*, 2022, **110**, 2542–2573.
200 V. Falanga, R. R. Isseroff, A. M. Soulika, M. Romanelli, D. Margolis, S. Kapp, M. Granick and K. Harding, *Nat. Rev. Dis. Primers*, 2022, **8**, 50.
201 P. Monika, M. N. Chandraprabha, A. Rangarajan, P. V. Waiker and K. N. Chidambara Murthy, *Front. Nutr.*, 2022, **8**, 791899.

202 B. Bhar, D. Chouhan, N. Pai and B. B. Mandal, *ACS Appl. Bio Mater*, 2021, **4**, 7738–7763.
203 C. Wiegand, U. C. Hipler, P. Elsner and J. Tittelbach, *Chronic Wound Care Manag. Res.*, 2015, **2**, 101–111.
204 G. Han and R. Ceilley, *Adv. Ther*, 2017, **34**, 599–610.
205 D. Simões, S. P. Miguel, M. P. Ribeiro, P. Coutinho, A. G. Mendonca and I. J. Correia, *Eur. J. Pharm. Biopharm.*, 2018, **127**, 130–141.
206 M. Farahani and A. Shafiee, *Adv. Healthc. Mater*, 2021, **10**, 2100477.
207 P. Dhivya, V. V. Padma and E. Santhini, *BioMedicine*, 2015, **5**, 24–28.
208 Y. Xiong, Q. Feng, L. Lu, K. Zha, T. Yu, Z. Lin, Y. Hu, A. C. Panayi, V. N. Ziahmagi, X. Chu, L. Chen, M. A. Shahbazi, B. Mi and G. Liu, *Adv. Funct. Mater.*, 2023, **33**, 2213066.
209 Z. Xiao, S. Zhao, X. Zhang, G. Wei and Z. Su, *Macromol. Mater. Eng.*, 2022, **307**, 2200385.
210 G. Kaur, G. Narayanan, D. Garg, A. Sachdev and I. Matai, *ACS Appl. Bio Mater*, 2022, **5**, 2069–2106.
211 T. Guan, J. Li, C. Chen and Y. Liu, *Adv. Sci*, 2022, **9**, 2104165.
212 R. Binaymotlagh, L. Chronopoulou, F. H. Haghighi, I. Fratoddi and C. Palocci, *Materials*, 2022, **15**, 5871.
213 R. Jayakumar, M. Prabaharan, K. P. T. Sudheesh, S. V. Nair and H. Tamura, *Biotechnol. Adv.*, 2011, **29**, 322–337.
214 G. Augustine, M. Aarthy, H. Thiagarajan, S. Selvaraj, N. R. Kamini, G. Shanmugam and N. Ayyadurai, *Adv. Healthc. Mater*, 2021, **10**, 2001832.
215 X. Du, J. Zhou, J. Shi and B. Xu, *Chem. Rev.*, 2015, **115**, 13165–13307.
216 D. Seliktar, *Science*, 2012, **336**, 1124–1128.
217 G. Huang, F. Li, X. Zhao, Y. Ma, Y. Li, M. Lin, G. Jin, T. J. Lu, G. M. Genin and F. Xu, *Chem. Rev.*, 2017, **117**, 12764–12850.
218 K. Y. Lee and D. J. Mooney, *Chem. Rev.*, 2001, **101**, 1869–1880.
219 Y. Osada and J. P. Gong, *Adv. Mater.*, 1998, **10**, 827–837.
220 Y. Kamiyama, R. Tamate, T. Hiroi, S. Samitsu, K. Fujii and T. Ueki, *Sci. Adv.*, 2022, **8**, eadd0226.
221 S. Bhattacharya and S. K. Samanta, *Chem. Rev.*, 2016, **116**, 11967–12028.
222 D. A. Gyles, L. D. Castro, J. O. C. Silva and R. M. Ribeiro-Costa, *Eur. Polym. J.*, 2017, **88**, 373–392.
223 U. S. K. Madduma-Bandarage and S. V. Madihally, *J. Appl. Polym. Sci.*, 2021, **138**, 50376.
224 M. Patenaude and T. Hoare, *Biomacromolecules*, 2012, **13**, 369–378.
225 L. Wang, D. Chen, K. Jiang and G. Shen, *Chem. Soc. Rev.*, 2017, **46**, 6764–6815.
226 M. Irimia-Vladu, *Chem. Soc. Rev.*, 2014, **43**, 588–610.
227 M. Smith and S. Kar-Narayan, *Int. Mater. Rev.*, 2022, **67**, 65–88.
228 I. Apsite, S. Salehi and L. Ionov, *Chem. Rev.*, 2022, **122**, 1349–1415.
229 M. Smith and S. Kar-Narayan, *Int. Mater. Rev.*, 2022, **67**, 65.
230 K. K. Sappati and S. Bhadra, *Sensors*, 2018, **18**, 3605.
231 Y. Osada and J. Gong, *Prog. Polym. Sci.*, 1993, **18**, 187–226.
232 K. Zhang, Q. Feng, Z. Fang, L. Gu and L. Bian, *Chem. Rev.*, 2021, **121**, 11149–11193.
233 B. Salahuddin, S. Wang, D. Sangian, S. Aziz and Q. Gu, *ACS Appl. Bio Mater*, 2021, **4**, 2886–2906.
234 Y. Zhao, S. Song, X. Ren, J. Zhang, Q. Lin and Y. Zhao, *Chem. Rev.*, 2022, **122**, 5604–5640.
235 H. Montazerian, E. Davoodi, A. Baidya, S. Baghdasarian, E. Sarikhani, C. E. Meyer, R. Haghniaz, M. Badv, N. Annabi, A. Khademhosseini and P. S. Weiss, *Chem. Rev.*, 2022, **122**, 12864–12903.
236 W. Liu, M. A. Heinrich, Y. Zhou, A. Akpek, N. Hu, X. Liu, X. Guan, Z. Zhong, X. Jin, A. Khademhosseini and Y. S. Zhang, *Adv. Healthcare Mater*, 2017, **6**, 1601451.
237 F. Gao, Z. Xu, Q. Liang, H. Li, L. Peng, M. Wu, X. Zhao, X. Cui, C. Ruan and W. Liu, *Adv. Sci*, 2019, **6**, 1900867.
238 D. Chimene, R. Kaunas and A. K. Gaharwar, *Adv. Mater.*, 2020, **32**, 1902026.
239 H. Thakar, S. M. Sebastian, S. Mandal, A. Pople, G. Agarwal and A. Srivastava, *ACS Biomater. Sci. Eng*, 2019, **5**, 6320–6341.
240 S. V. Vlierberghe, P. Dubruel and E. Schacht, *Biomacromolecules*, 2011, **12**, 1387–1408.
241 J. K. Wychowaniec and D. F. Brougham, *Adv. Sci.*, 2022, **9**, 2202278.
242 L. Bai, L. Liu, M. Esquivel, B. L. Tardy, S. Huan, X. Niu, S. Liu, G. Yang, Y. Fan and O. J. Rojas, *Chem. Rev.*, 2022, **122**, 11604–11674.
243 S. K. Ghosh, P. Adhikary, S. Jana, A. Biswas, V. Sencadas, S. D. Gupta, B. Tudu and D. Mandal, *Nano Energy*, 2017, **36**, 166–175.
244 S. K. Ghosh and D. Mandal, *ACS Sustainable Chem. Eng*, 2017, **5**, 8836–8843.
245 X. Yang, Y. Jia, K. Yao, Y. Wang and J. Ma, *J. Appl. Polym. Sci.*, 1996, **62**, 2351–2354.
246 M. Mohseni, S. A. A. Ramazani, F. H. Shirazi and N. H. Nemati, *Mater. Today Commun*, 2021, **26**, 101785.
247 S. F. A. Zaidi, A. Saeed, J. H. Heo and J. H. Lee, *J. Mater. Chem. A*, 2023, **11**, 13844–13875.
248 W. R. Li, C. H. Li, G. Z. Zhang, L. K. Li, K. Huang, X. T. Gong, C. Zhang, A. Zheng, Y. X. Tang, Z. Z. Wang, Q. L. Tong, W. Dong, S. L. Jiang, S. L. Zhang and Q. Wang, *Adv. Mater.*, 2021, **33**, 2104107.
249 D. Son, J. Lee, S. Qiao, R. Ghaffari, J. Kim, J. E. Lee, C. Song, S. J. Kim, D. J. Lee, S. W. Jun, S. Yang, M. Park, J. Shin, K. Do, M. Lee, K. Kang, C. S. Hwang, N. Lu, T. Hyeon and D. H. Kim, *Nat. Nanotechnol*, 2014, **9**, 397.
250 Z. Lei, Q. Wang, S. Sun, W. Zhu and P. Wu, *Adv. Mater.*, 2017, **29**, 1700321.
251 X. Wang, L. Dong, H. Zhang, R. Yu, C. Pan and Z. L. Wang, *Adv. Sci*, 2015, **2**, 1500169.
252 M. L. Hammock, A. Chortos, B. C. K. Tee, J. B. H. Tok and Z. Bao, *Adv. Mater.*, 2013, **25**, 5997–6038.
253 Y. Dobashi, D. Yao, Y. Petel, T. N. Nguyen, M. S. Sarwar, Y. Thabet, C. L. W. Ng, E. S. Glitz, G. T. M. Nguyen,

C. Plesse, F. Vidal, C. A. Michal and J. D. W. Madden, *Science*, 2022, **376**, 502–507.
254 Z. Jiang and P. Song, *Science*, 2022, **376**, 245.
255 J. Odent, N. Baleine, V. Biard, Y. Dobashi, C. Vancaeyzeele, G. T. M. Nguyen, J. D. W. Madden, C. Plesse and J. M. Raquez, *Adv. Funct. Mater.*, 2023, **33**, 2210485.
256 Z. W. K. Low, Z. Li, C. Owh, P. L. Chee, E. Ye, K. Dan, S. Y. Chan, D. J. Young and X. J. Loh, *Biomater. Sci*, 2020, **8**, 776–797.
257 Y. Cheng, Y. Ma, L. Li, M. Zhu, Y. Yue, W. Liu, L. Wang, S. Jia, C. Li, T. Qi, J. Wang and Y. Gao, *ACS Nano*, 2020, **14**, 2145–2155.
258 X. Shi, X. Fan, Y. Zhu, Y. Liu, P. Wu, R. Jiang, B. Wu, H. A. Wu, H. Zheng, J. Wang, X. Ji, Y. Chen and J. Liang, *Nat. Commun.*, 2022, **13**, 1119.
259 C. Wan, L. Zhang, K. T. Yong, J. Lid and Y. Wu, *J. Mater. Chem. C*, 2021, **9**, 11001–11029.
260 S. Zhao and J. H. Ahn, *Mater. Sci. Eng. R*, 2022, **148**, 100672.
261 S. Mishra, S. Mohanty and A. Ramadoss, *ACS Sens*, 2022, **7**, 2495–2520.
262 G. Li, C. Li, G. Li, D. Yu, Z. Song, H. Wang, X. Liu, H. Liu and W. Liu, *Small*, 2022, **18**, 2101518.
263 J. Fu, Q. Sun, C. Long, X. Hu, N. Wang, H. Guo, W. Zeng, Y. Xiong and N. Wei, *J. Mater. Sci.*, 2022, **57**, 3553–3564.
264 H. Li, M. Long, H. Su, L. Tan, X. Shi, Y. Du, Y. Luo and H. Deng, *Carbohydr. Polym*, 2022, **290**, 119482.
265 S. G. Alamdari, A. Alibakhshi, M. de la Guardia, B. Baradaran, R. Mohammadzadeh, M. Amini, P. Kesharwani, A. Mokhtarzadeh, F. Oroojalian and A. Sahebkar, *Adv. Healthcare Mater*, 2022, **11**, 2200526.
266 R. M. Fu, L. J. Tu, Y. H. Zhou, L. Fan, F. M. Zhang, Z. G. Wang, J. Xing, D. F. Chen, C. L. Deng, G. X. Tan, P. Yu, L. Zhou and C. Y. Ning, *Chem. Mater.*, 2019, **31**, 9850–9860.
267 W. Zhao, Z. Shi, S. Hu, G. Yang and H. Tian, *Adv. Compos. Hybrid Mater*, 2018, **1**, 320–331.
268 E. Scarpa, V. M. Mastronardi, F. Guido, L. Algieri, A. Qualtieri, R. Fiammengo, F. Rizzi and M. De Vittorio, *Sci. Rep.*, 2020, **10**, 10854.
269 C. Wang, Y. Hu, Y. Liu, Y. Shan, X. Qu, J. Xue, T. He, S. Cheng, H. Zhou, W. Liu, Z. H. Guo, W. Hua, Z. Liu, Z. Li and C. Lee, *Adv. Funct. Mater.*, 2023, 2303696.
270 K. Kang, H. Jung, S. An, H. W. Baac, M. Shin and D. Son, *Polymers*, 2021, **13**, 3272.
271 C. Jia, Y. Zhu, F. Sun, T. Zhao, R. Xing, Y. Mao and C. Zhao, *Electronics*, 2021, **10**, 2584.
272 Y. Zhu, F. Sun, C. Jia, T. Zhao and Y. Mao, *Nanomaterials*, 2021, **12**, 104.
273 S. Veeralingam and S. Badhulika, *Mater. Res. Bull.*, 2022, **150**, 111779.
274 T. Abu Ali, P. Schäffner, M. Belegratis, G. Schider, B. Stadlober and A. M. Coclite, *Adv. Mater. Technol.*, 2022, **7**, 2200246.
275 Z. Hu, J. Li, X. Wei, C. Wang, Y. Cao, Z. Gao, J. Han and Y. Li, *ACS Appl. Mater. Interfaces*, 2022, **14**, 45853–45868.
276 Y. Wang, Y. Xie, X. Xie, D. Wu, H. Wu, X. Luo, Q. Wu, L. Zhao and J. Wu, *Adv. Funct. Mater.*, 2023, **33**, 2210224.
277 J. Liang, H. Zeng, L. Qiao, H. Jiang, Q. Ye, Z. Wang, B. Liu and Z. Fan, *ACS Appl. Mater. Interfaces*, 2022, **14**, 30507–30522.
278 L. Wang, Y. Yu, X. Zhao, Z. Zhang, X. Yuan, J. Cao, W. Meng, L. Ye, W. Lin and G. Wang, *ACS Appl. Mater. Interfaces*, 2022, **14**, 46273–46289.
279 S. Du, N. Zhou, Y. Gao, G. Xie, H. Du, H. Jiang, L. Zhang, J. Tao and J. Zhu, *Nano Res*, 2020, **13**, 2525–2533.
280 M. Mohseni, F. Delavar and H. Rezaei, *J. Macromol. Sci. Part A*, 2021, **58**, 694–708.
281 G. Yu, Y. Zhang, Q. Wang, N. Dan, Y. Chen, Z. Li, W. Dan and Y. Wang, *Ind. Eng. Chem. Res.*, 2023, **62**, 5468–5481.
282 J. Wu, T. Chen, Y. Wang, J. Bai, C. Lao, M. Luo, M. Chen, W. Peng, W. Zhi, J. Weng and J. Wang, *Biomedicines*, 2022, **10**, 1165.
283 D. Jackson, A. M. Sarki, R. Betteridge and J. Brooke, *Int. J. Nurs. Stud.*, 2019, **92**, 109–120.
284 M. E. Posthauer, M. Banks, B. Dorner and J. M. Schols, *Adv. Ski. Wound Care*, 2015, **28**, 175–188.
285 J. S. Mervis and T. J. Phillips, *J. Am. Acad. Dermatol.*, 2019, **81**, 881–890.
286 B. Hajhosseini, M. T. Longaker and G. C. Gurtner, *Ann. Surg.*, 2020, **271**, 671–679.
287 B. Barrois, F. A. Allaert and D. Colin, *J. Wound Care*, 1995, **4**, 234–236.
288 J. Alderden, J. Rondinell, G. Pepper, M. Cummins and J. Whitney, *Int. J. Nurs. Stud*, 2017, **71**, 97–114.
289 W. V. Padula and B. A. Delarmente, *Int. Wound J*, 2019, **16**, 634–640.
290 A. Gefen, P. Alves, G. Ciprandi, F. Coyer, C. T. Milne, K. Ousey, N. Ohura, N. Waters and P. Worsley, *J. Wound Care*, 2020, **29**, S1–S52.
291 Y. Meng, H. Zhao, Z. G. Yin, X. N. Qi and S. B. Tsai, *Math. Probl. Eng.*, 2021, **2021**, 5570533.
292 L. McNichol, D. Mackey, C. Watts and N. Zuecca, *Nursing*, 2020, **50**, 41–44.
293 A. Gefen, *Int. Wound J*, 2022, **19**, 1797–1809.
294 Y. Jin, J. Li, S. Wu and F. Zhou, *Medicine (Baltimore)*, 2021, **100**, e24165.
295 C. Forni, D. Gazineo, E. Allegrini, T. Bolgeo, A. Brugnolli, F. Canzan, P. Chiari, A. Evangelista, A. M. Grugnetti, G. Grugnetti, M. Guberti, M. Matarese, E. Mezzalira, L. Pierboni, L. Prosperi, B. Sofritti, C. Tovazzi, S. Vincenzi, P. Zambiasi, C. Zoffoli, E. Ambrosi, F. Bandi, M. Batani, G. Bertin, L. Bianchi, M. Carmagnini, S. Cedioli, S. Colognese, M. Consuelo, F. D'Alessandro, M. Fontana, L. Galassi, M. Gridelli, P. Magnani, M. Morri, B. Ortolani, M. Scialla, P. Stanga, P. Toselli and S. Zanelli, *Int. J. Nurs. Stud.*, 2022, **127**, 104172.
296 A. Grigatti and A. Gefen, *Int. Wound J*, 2022, **19**, 515–530.
297 A. Grigatti and A. Gefen, *Int Wound J*, 2022, **19**, 1051–1063.
298 A. Gefen, *Int Wound J*, 2022, **19**, 1797–1809.
299 C. H. Li, C. R. Xiao, L. Z. Zhan, Z. K. Zhang, J. Xing, J. X. Zhai, Z. N. Zhou, G. X. Tan, J. H. Piao, Y. H. Zhou, S. J. Qi, Z. G. Wang, P. Yu and C. Y. Ning, *Bioact. Mater*, 2022, **18**, 399–408.

300 S. Ghosh, W. Qiao, Z. Yang, S. Orrego and P. Neelakantan, *J. Funct. Biomater*, 2023, **14**, 8.
301 Y. Li, R. Fu, Y. Guan, Z. Zhang, F. Yang, C. Xiao, Z. Wang, P. Yu, L. Hu, Z. Zhou and C. Ning, *ACS Biomater. Sci. Eng.*, 2022, **8**, 3078–3086.
302 Z. L. Wang and W. Wu, *Angew. Chem., Int. Ed.*, 2012, **51**, 11700–11721.
303 Y. Bai, H. Jantunen and J. Juuti, *Front. Mater*, 2018, **5**, 65.
304 W. Qian, H. Wu and Y. Yang, *Adv. Electron. Mater*, 2022, **8**, 2200190.
305 B. H. Park, B. S. Kang, S. D. Bu, T. W. Noh, J. Lee and W. Jo, *Nature*, 1999, **401**, 682–684.
306 S. T. Han, Y. Zhou and V. A. L. Roy, *Adv. Mater.*, 2013, **25**, 5425–5449.
307 G. H. Haertling, *J. Am. Ceram. Soc.*, 1999, **82**, 797–818.
308 J. Hoffman, X. Pan, J. W. Reiner, F. J. Walker, J. P. Han, C. H. Ahn and T. P. Ma, *Adv. Mater.*, 2010, **22**, 2957–2961.
309 S. Y. Yang, J. Seidel, S. J. Byrnes, P. Shafer, C. H. Yang, M. D. Rossell, P. Yu, Y. H. Chu, J. F. Scott, J. W. Ager, L. W. Martin and R. Ramesh, *Nat. Nanotechnol*, 2010, **5**, 143–147.
310 F. R. Fan, W. Tang and Z. L. Wang, *Adv. Mater.*, 2016, **28**, 4283–4305.
311 X. Lv, J. G. Zhu, D. Q. Xiao, X. X. Zhang and J. G. Wu, *Chem. Soc. Rev.*, 2020, **49**, 671–707.
312 S. Xu, Y. Qin, C. Xu, Y. Wei, R. Yang and Z. L. Wang, *Nat. Nanotechnol*, 2010, **5**, 366–373.
313 A. Rovisco, A. dos Santos, T. Cramer, J. Martins, R. Branquinho, H. Águas, B. Fraboni, E. Fortunato, R. Martins, R. Igreja and P. Barquinha, *ACS Appl. Mater. Interfaces*, 2020, **12**, 18421–18430.
314 M. Acosta, N. Novak, V. Rojas, S. Patel, R. Vaish, J. Koruza, G. A. Rossetti and J. Rödel, *Appl. Phys. Rev.*, 2017, 4, 041305.
315 P. Snapp, C. Cho, D. Lee, M. F. Haque, S. W. Nam and C. Park, *Adv. Mater.*, 2020, **32**, 2004607.
316 T. Li and P. S. Lee, *Small Struct*, 2022, **3**, 2100128.
317 K. Park, C. K. Jeong, J. Ryu, G. T. Hwang and K. J. Lee, *Adv. Energy Mater*, 2013, **3**, 1539–1544.
318 G. Clementi, F. Cottone, A. D. Michele, L. Gammaitoni, M. Mattarelli, G. Perna, M. L. Suárez, S. Baglio, C. Trigona and I. Neri, *Energies*, 2022, **15**, 6227.
319 S. Mishra, L. Unnikrishnan, S. K. Nayak and S. Mohanty, *Macromol. Mater. Eng.*, 2019, **304**, 1800463.
320 K. I. Park, S. Xu, Y. Liu, G. T. Hwang, S. J. L. Kang, Z. L. Wang and K. J. Lee, *Nano Lett*, 2010, **10**, 4939–4943.
321 J. Wu, D. Xiao and J. Zhu, *Chem. Rev.*, 2015, **115**, 2559–2595.
322 K. I. Park, M. Lee, Y. Liu, S. Moon, G. T. Hwang, G. Zhu, J. E. Kim, S. O. Kim, D. K. Kim, Z. L. Wang and K. J. Lee, *Adv. Mater.*, 2012, **24**, 2999–3004.
323 D. Zhao, Y. Zhu, W. Cheng, W. Chen, Y. Wu and H. Yu, *Adv. Mater.*, 2021, **33**, 2000619.
324 J. Min, J. Tu, C. Xu, H. Lukas, S. Shin, Y. Yang, S. A. Solomon, D. Mukasa and W. Gao, *Chem. Rev.*, 2023, **123**, 5049–5138.
325 N. Sezer and M. Koç, *Nano Energy*, 2021, **80**, 105567.
326 J. H. Guo, G. W. Skinner, W. W. Harcum and P. E. Barnum, *Pharm. Sci. Technol. Today*, 1998, **1**, 254–261.
327 M. Teodorescu and M. Bercea, *Polym. Plast. Technol. Eng*, 2015, **54**, 923–943.
328 Y. Luo, Y. Hong, L. Shen, F. Wu and X. Lin, *AAPS PharmSciTech*, 2021, **22**, 34.
329 P. Franco and I. D. Marco, *Polymers*, 2020, **12**, 1114.
330 J. Sun, Y. Wang, S. Dou, C. Ruan and C. Hu, *Materials Letters*, 2012, **67**, 215–218.
331 H. GhaedRahmati, M. Frounchi and S. Dadbin, *Mater. Sci. Eng., B*, 2022, **276**, 115535.
332 X. Wang, X. Dai and Y. Chen, *Small*, 2023, 2301693.
333 R. Fu, X. Zhong, C. Xiao, J. Lin, Y. Guan, Y. Tian, Z. Zhou, G. Tan, H. Hu, L. Zhou and C. Ning, *Nano Energy*, 2023, **114**, 108617.
334 G. Han and R. Ceilley, *Adv Ther*, 2017, **34**, 599–610.
335 C. K. Sen, *Adv. Wound Care*, 2021, **10**, 281–292.
336 D. Huang, Y. Cheng, G. Chen and Y. Zhao, *Research*, 2023, **6**, 0022.
337 A. Mahler, M. Reches, M. Rechter, S. Cohen and E. Gazit, *Adv. Mater.*, 2006, **18**, 1365–1370.
338 V. Jayawarna, M. Ali, T. A. Jowitt, A. E. Miller, A. Saiani, J. E. Gough and R. V. Ulijn, *Adv. Mater.*, 2006, **18**, 611–614.
339 M. Amit, S. Yuran, E. Gazit, M. Reches and N. Ashkenasy, *Adv. Mater.*, 2018, **30**, 1707083.
340 A. M. Smith, R. J. Williams, C. Tang, P. Coppo, R. F. Collins, M. L. Turner, A. Saiani and R. V. Ulijn, *Adv. Mater.*, 2008, **20**, 37–41.
341 L. Adler-Abramovich and E. Gazit, *Chem. Soc. Rev.*, 2014, **43**, 6881–6893.
342 S. Fleming and R. V. Ulijn, *Chem. Soc. Rev.*, 2014, **43**, 8150–8177.
343 M. Frenkel-Pinter, M. Samanta, G. Ashkenasy and L. J. Leman, *Chem. Rev.*, 2020, **120**, 4707–4765.
344 X. Yan, P. Zhu and J. Li, *Chem. Soc. Rev.*, 2010, **39**, 1877–1890.
345 C. Yan and D. J. Pochan, *Chem. Soc. Rev.*, 2010, **39**, 3528–3540.
346 J. Raeburn, A. Z. Cardoso and D. J. Adams, *Chem. Soc. Rev.*, 2013, **42**, 5143–5156.
347 N. M. Sangeetha and U. Maitra, *Chem. Soc. Rev.*, 2005, **34**, 821–836.
348 S. Panja and D. J. Adams, *Chem. Soc. Rev.*, 2021, **50**, 5165–5200.
349 A. Levin, T. A. Hakala, L. Schnaider, G. J. L. Bernardes, E. Gazit and T. P. J. Knowles, *Nat. Rev. Chem*, 2020, **4**, 615–634.
350 E. Prince and E. Kumacheva, *Nat. Rev. Mater*, 2019, **4**, 99–115.
351 L. Shi, P. Ding, Y. Wang, Y. Zhang, D. Ossipov and J. Hilborn, *Macromol. Rapid Commun.*, 2019, **40**, e1800837.
352 S. C. Lee, G. Gillispie, P. Prim and S. J. Lee, *Chem. Rev.*, 2020, **120**, 10834–10886.
353 X. Zhang, Y. Tang, P. Wang, Y. Wang, T. Wu, T. Li, S. Huang, J. Zhang, H. Wang, S. Ma, L. Wang and W. Xu, *New J. Chem*, 2022, **46**, 13838–13855.

354 Y. Zheng, N. Tang, R. Omar, Z. Hu, T. Duong, J. Wang, W. Wu and H. Haick, *Adv. Funct. Mater.*, 2021, **31**, 2105482.
355 Y. Wang, H. Haick, S. Guo, C. Wang, S. Lee, T. Yokota and T. Someya, *Chem. Soc. Rev.*, 2022, **51**, 3759–3793.
356 Q. Li, L. Chen, M. Guo and Z. Hu, *Adv. Mater. Technol.*, 2021, **7**, 2101371.
357 J. Lu, S. Hu, W. Li, X. Wang, X. Mo, X. Gong, H. Liu, W. Luo, W. Dong, C. Sima, Y. Wang, G. Yang, J. T. Luo, S. Jiang, Z. Shi and G. Zhang, *ACS Nano*, 2022, **16**, 3744–3755.
358 P. Wang, M. Hu, H. Wang, Z. Chen, Y. Feng, J. Wang, W. Ling and Y. Huang, *Adv. Sci*, 2020, **7**, 2001116.
359 P. K. Annamalai, A. K. Nanjundan, D. P. Dubal and J. B. Baek, *Adv. Mater. Technol.*, 2021, **6**, 2001164.
360 S. Maiti, S. K. Karan, J. K. Kim and B. B. Khatua, *Adv. Energy Mater*, 2019, **9**, 1803027.
361 W. Ji, B. Xue, Y. Yin, S. Guerin, Y. Wang, L. Zhang, Y. Cheng, L. J. W. Shimon, Y. Chen, D. Thompson, R. Yang, Y. Cao, W. Wang, K. Cai and E. Gazit, *J. Am. Chem. Soc.*, 2022, **144**, 18375–18386.
362 J. O'Donnell, S. Guerin, P. Makam, P. A. Cazade, E. U. Haq, K. Tao, E. Gazit, C. Silien, T. Soulimane, D. Thompson and S. A. M. Tofail, *Appl. Mater. Today*, 2020, **21**, 100818.
363 A. Kholkin, N. Amdursky, I. Bdikin, E. Gazit and G. Rosenman, *ACS Nano*, 2010, **4**, 610–614.
364 S. Bera, P. A. Cazade, S. Bhattacharya, S. Guerin, M. Ghosh, F. Netti, D. Thompson and L. Adler-Abramovich, *ACS Appl. Mater. Interfaces*, 2022, **14**, 46827–46840.
365 W. Ji, B. Xue, S. Bera, S. Guerin, Y. Liu, H. Yuan, Q. Li, C. Yuan, L. J. W. Shimon, Q. Ma, E. Kiely, S. A. M. Tofail, M. Si, X. Yan, Y. Cao, W. Wang, R. Yang, D. Thompson, J. Li and E. Gazit, *ACS Nano*, 2020, **14**, 10704–10715.
366 W. Ji, H. Yuan, B. Xue, S. Guerin, H. Li, L. Zhang, Y. Liu, L. J. W. Shimon, M. Si, Y. Cao, W. Wang, D. Thompson, K. Cai, R. Yang and E. Gazit, *Angew. Chem., Int. Ed.*, 2022, **61**, e202201234.
367 Y. Huo, J. Hu, Y. Yin, P. Liu, K. Cai and W. Ji, *ChemBioChem*, 2023, **24**, e202200582.
368 S. Guerin, S. A. M. Tofail and D. Thompson, *Cryst. Growth Des.*, 2018, **18**, 4844–4848.
369 E. D. Sødahl, J. Walker and K. Berland, *Cryst. Growth Des.*, 2023, **23**, 729–740.
370 C. R. Bernardo, R. M. F. Baptista, E. de Matos Gomes, P. E. Lopes, M. M. M. Raposo, S. P. G. Costa and M. S. Belsley, *Nanoscale Adv*, 2020, **2**, 1206–1213.
371 R. M. F. Baptista, P. E. Lopes, A. R. O. Rodrigues, N. Cerca, M. S. Belsley and E. de Matos Gomes, *Mater. Adv.*, 2022, **3**, 2934–2944.
372 K. Tao, A. Levin, L. Adler-Abramovich and E. Gazit, *Chem. Soc. Rev.*, 2016, **45**, 3935–3953.
373 A. Lampel, R. V. Ulijn and T. Tuttle, *Chem. Soc. Rev.*, 2018, **47**, 3737–3758.
374 C. Yuan, W. Ji, R. Xing, J. Li, E. Gazit and X. Yan, *Nat. Rev. Chem*, 2019, **3**, 567–588.
375 L. M. D. Rodriguez, Y. Hemar, J. Cornish and M. A. Brimble, *Chem. Soc. Rev.*, 2016, **45**, 4797–4824.
376 K. Ryan, J. Beirne, G. Redmond, J. I. Kilpatrick, J. Guyonnet, N. V. Buchete, A. L. Kholkin and B. J. Rodriguez, *ACS Appl. Mater. Interfaces*, 2015, **7**, 12702–12707.
377 J. Raeburn, C. Mendoza-Cuenca, B. N. Cattoz, M. A. Little, A. E. Terry, A. Z. Cardoso, P. C. Griffiths and D. J. Adams, *Soft Matter*, 2015, **11**, 927–935.
378 C. H. Görbitz, *Chem. Eur. J*, 2007, **13**, 1022–1031.
379 Y. Huang, X. Fan, S. C. Chen and N. Zhao, *Adv. Funct. Mater.*, 2019, **29**, 1808509.
380 F. Narita and M. Fox, *Adv. Eng. Mater.*, 2018, **20**, 1700743.
381 G. Finkelstein-Zuta, R. Shitrit, S. Gilead, S. Rencus-Lazar and E. Gazit, *Isr. J. Chem.*, 2022, **62**, e20220002.
382 Y. Wu, Y. Luo, T. J. Cuthbert, A. V. Shokurov, P. K. Chu, S. P. Feng and C. Menon, *Adv. Sci*, 2022, **9**, 2106008.
383 Z. L. Wang, *Nano Res*, 2008, **1**, 1–8.
384 C. Dagdeviren, P. Joe, O. L. Tuzman, K. I. Park, K. J. Lee, Y. Shi, Y. G. Huang and J. A. Rogers, *Extreme Mech. Lett.*, 2016, **9**, 269–281.
385 M. Yu, Y. Peng, X. Wang and F. Ran, *Adv. Funct. Mater.*, 2023, 2301877.
386 F. Mokhtari, Z. Cheng, C. H. Wang and J. Foroughi, *Global Challenges*, 2023, **7**, 2300019.
387 D. H. Kim, H. J. Shin, H. Lee, C. K. Jeong, H. Park, G. T. Hwang, H. Y. Lee, D. J. Joe, J. H. Han, S. H. Lee, J. Kim, B. Joung and K. J. Lee, *Adv. Funct. Mater.*, 2017, **27**, 1700341.
388 Y. Liu, H. Khanbareh, M. A. Halim, A. Feeney, X. Zhang, H. Heidari and R. Ghannam, *Nano Select*, 2021, **2**, 1459–1479.
389 J. Zhao, R. Ghannam, K. O. Htet, Y. Liu, M. K. Law, V. A. L. Roy, B. Michel, M. A. Imran and H. Heidari, *Adv. Healthcare Mater*, 2020, **9**, 2000779.
390 S. Chen, P. Zhu, L. Mao, W. Wu, H. Lin, D. Xu, X. Lu and J. Shi, *Adv. Mater.*, 2023, **35**, 2208256.
391 B. Shi, Z. Li and Y. Fan, *Adv. Mater.*, 2018, **30**, 1801511.
392 G. T. Hwang, M. Byun, C. K. Jeong and K. J. Lee, *Adv. Healthcare Mater*, 2015, **4**, 646–658.
393 Q. Zheng, B. Shi, Z. Li and Z. L. Wang, *Adv. Sci*, 2017, **4**, 1700029.
394 F. Ali, W. Raza, X. Li, H. Gul and K. H. Kim, *Nano Energy*, 2019, **57**, 879–902.
395 D. Jiang, B. Shi, H. Ouyang, Y. Fan, Z. L. Wang and Z. Li, *ACS Nano*, 2020, **14**, 6436–6448.
396 S. Azimi, A. Golabchi, A. Nekookar, S. Rabbani, M. H. Amiri, K. Asadi and M. M. Abolhasani, *Nano Energy*, 2021, **83**, 105781.
397 G. T. Hwang, H. Park, J. H. Lee, S. Oh, K. I. Park, M. Byun, H. Park, G. Ahn, C. K. Jeong, K. No, H. Kwon, S. G. Lee, B. Joung and K. J. Lee, *Adv. Mater.*, 2014, **26**, 4880–4887.